/5320

...rvices Technical Information Agency

Reproduced by

...OCUMENT SERVICE CENTER

KNOTT BUILDING, DAYTON, 2, OHIO

...CLASSIFIED

NAVORD REPORT 3854

FC

A THEORETICAL INVESTIGATION OF TURBULENT BOUNDARY LAYER FLOW WITH HEAT TRANSFER AT SUPERSONIC AND HYPERSONIC SPEEDS

19 MAY 1955

U. S. NAVAL ORDNANCE LABORATORY
WHITE OAK, MARYLAND

NAVORD Report 3854

Aeroballistic Research Report 258

A THEORETICAL INVESTIGATION OF TURBULENT BOUNDARY LAYER FLOW WITH HEAT TRANSFER AT SUPERSONIC AND HYPERSONIC SPEEDS

Prepared by:

Jerome Persh

ABSTRACT: A theoretical investigation of compressible turbulent boundary layer flow with and without steady state heat transfer has been conducted. This investigation is based on a simple physical model of the flow suggested first by Prandtl and used later by Donaldson. The physical model consists of a laminar sublayer region with a linear velocity profile and an outer turbulent portion with a power law velocity profile. Comparisons between theory and experiment demonstrate that the analysis yields good results for compressible turbulent boundary layer flow with and without steady state heat transfer.

U. S. NAVAL ORDNANCE LABORATORY
WHITE OAK, MARYLAND

This report contains the results of a theoretical investigation of compressible turbulent boundary layer flow with and without steady state heat transfer. The significance of this work is apparent when it is considered that although a great deal of experimental and theoretical information exists for supersonic turbulent boundary layers in the absence of heat transfer, there are relatively few detailed investigations in the supersonic and hypersonic speed ranges that include the effects of heat transfer.

The work was jointly sponsored by the U. S. Naval Bureau of Ordnance and the U. S. Air Force, and was performed under Tasks NOL-M9a-133-1-55 and NOL-M9a-133-5-55. The author is deeply indebted to Dr. R. E. Wilson and Dr. R. K. Lobb for their guidance and continued interest during the course of the investigation, and to Mrs. Leah Brown of the Applied Mathematics Division, who carried out the computation of the data contained in Table I.

JOHN T. HAYWARD
Captain, USN
Commander

H. H. KURZWEG, Chief
Aeroballistic Research Department
By direction

CONTENTS

ILLUSTRATIONS

SYMBOLS

c_f = Local skin friction coefficient based on free-stream conditions, $2\tau_w/\rho_\infty u_\infty^2$

C_F = Mean skin friction coefficient based on free-stream conditions, $\frac{2D}{\rho_\infty u_\infty^2 x}$

c_{fi} = Incompressible local skin friction coefficient for zero heat transfer based on free-stream conditions

C_{Fi} = Incompressible mean skin friction coefficient for zero heat transfer based on free-stream conditions

D = Drag force

H = Boundary layer shape parameter, δ^*/θ

k = Constant in mixing length law

ℓ = Mixing length

M = Mach number

n = Exponent in power law velocity profile representation

r = Ratio of total shear stress to viscous shear stress

r.f. = Recovery factor

Re = Reynolds number

T = Local static temperature

u = Mean velocity component in x-direction

u^+ = Velocity parameter, u/u_τ (based on wall conditions)

u_τ = Friction velocity $\sqrt{\tau_w/\rho_w}$

x = Axial distance along surface

y = Distance perpendicular to surface

y^+ = Wall distance parameter, yu_τ/ν (based on wall conditions)

SYMBOLS (continued)

δ = Total boundary layer thickness

δ^* = Boundary layer displacement thickness, $\int_0^\delta \left[1 - \frac{\rho u}{\rho_\infty u_\infty}\right] dy$

θ = Boundary layer momentum thickness, $\int_0^\delta \frac{\rho u}{\rho_\infty u_\infty} \left[1 - \frac{u}{u_\infty}\right] dy$

μ = Viscosity

ν = Kinematic viscosity

ρ = Density

$\tau_{Lam.}$ = Laminar shear stress

$\tau_{Turb.}$ = Turbulent shear stress

ω = Exponent in viscosity-temperature relationship

Subscripts:

e = Equilibrium wall temperature

L = Values at the edge of laminar sublayer

T = Turbulent region

w = Values based on wall conditions

x = Values based on distance from leading edge of plate

δ = Values based on boundary layer thickness

θ = Values based on boundary layer momentum thickness

∞ = Values based on free-stream conditions outside boundary layer

A THEORETICAL INVESTIGATION OF TURBULENT BOUNDARY LAYER FLOW WITH HEAT TRANSFER AT SUPERSONIC AND HYPERSONIC SPEEDS

INTRODUCTION

1. Despite a lack of experimental data, numerous formulae have been developed for the variation of turbulent skin friction on a flat plate, with and without steady state heat transfer. The reports of Rubesin, Maydew, and Varga (reference a), and Chapman and Kester (reference b) include good resumes of several theoretical treatments of this problem. All of the analyses reviewed in these references make use of empirical constants which are drawn from incompressible experimental data. Recent experimental results (reference c) have demonstrated that the empirical incompressible constants utilized are affected by heat transfer. Specifically, it has been found that the assumption that the edge of the laminar sublayer occurs at fixed values of the parameters u_L^+ (or y_L^+) is not strictly valid. Experimental results indicate that the value of u_L^+ does not only vary with heat transfer, but to some extent with Reynolds number and Mach number. It was felt, therefore, that a theoretical approach which is based on a realistic physical model of the flow, and which allows a prediction of the quantities at the edge of the laminar sublayer, is expedient at the present time.

2. Such an approach was originally devised by Prandtl (reference d) and recently extended to compressible flows by Donaldson (reference e) The physical model of a turbulent boundary layer proposed by these investigators may be briefly described as follows: It is assumed that the turbulent boundary layer velocity profile can be divided into two regions; the wall adjacent region called the laminar sublayer, where the velocity varies linearly with distance from the surface, and the outer turbulent portion, which is represented by a power profile. The intersection of these two profiles is defined as the edge of the laminar sublayer.

3. It is the purpose of this investigation to extend and revise the analysis of Donaldson in order to obtain consistency with the most recent and reliable experimental results for low speed turbulent boundary layers. The applicability of this analysis for compressible turbulent boundary layers with and without steady state heat transfer is demonstrated by comparisons with supersonic and hypersonic experimental results.

ANALYSIS

Incompressible Turbulent Boundary Layers

4. It has been established by numerous investigators that the velocity profile in the outer turbulent portion of the boundary layer may be adequately represented by a power profile of the form

$$\frac{u}{u_\infty} = \left[\frac{y}{\delta}\right]^{\frac{1}{n}} \qquad \delta_L \leq y \leq \delta \qquad (1)$$

while experimental evidence indicates that, in the laminar sublayer region, the velocity profile is essentially a straight line

$$\frac{u}{u_L} = \frac{y}{\delta_L} \times \text{constant} \qquad o \leq y \leq \delta_L \qquad (2)$$

The boundary layer is thus divided into a turbulent portion described by Eq. (1) and a laminar region having a linear velocity profile (Eq. 2). This is shown in Figure 1 with the real conditions in the transition region indicated by a dashed line.

5. Several general relations for the local skin friction coefficient can be deduced using the preceding postulates regarding the boundary layer velocity profile together with various assumptions regarding the shear stress at the edge of the laminar sublayer. These relations necessarily embody unknown functions which must be evaluated empirically.

6. Donaldson (reference e) introduced an empirical constant relating the total shear stress and the laminar shear stress in order to compute the skin friction. Taking

$$\frac{\tau_{Lam.} + \tau_{Turb.}}{\tau_{Lam.}} = r = \text{constant} \qquad (3)$$

and evaluating r at $y = \delta_L$ from the power profile given by Eq. (1), Donaldson (reference e) derived the following relation for the skin friction coefficient

$$c_{fi} = 2\left[\frac{n(r-1)}{k^2}\right]^{\frac{1-n}{1+n}}\left[\frac{1}{Re_\delta}\right]^{\frac{2}{n+1}} \qquad (4)$$

and evaluated the constant $(r-1)/k^2$ empirically using Blasius' (reference d) skin friction law. In Donaldson's analysis, the velocity profile exponent (n) is considered constant, and the Prandtl mixing length law

$$\ell = k\, y \tag{5}$$

is assumed in order to calculate the turbulent shear stress, $\tau_{Turb.}$*

7. In the present report the velocity profile exponent (n) was taken as a variable and the method by which Eq. (4) was correlated with experiment is as follows: First, Eq. (4) was equated to the Karman-Schoenherr incompressible skin friction law

$$c_{fi} = \frac{0.0568}{\left[\mathrm{Log}_{10}\,(2Re_\theta)\right]\left[\mathrm{Log}_{10}\,(2Re_\theta) + 0.868\right]} \tag{6}$$

which is regarded as a good representation of incompressible turbulent boundary layer skin friction coefficients over a wide Reynolds number range. This procedure yielded a variation of n with Re_θ. A comparison was then made between experimental data and the deduced variation of n with Re_θ. This approach seemed logical because the experimental variation of n with Re_θ is well

---

* An examination of Figure 2 suggests that since the shear stress is nearly constant near the wall, an alternate assumption regarding the relationship between the laminar and turbulent shear stress may be made. Within the sublayer the laminar shear stress predominates while outside the sublayer the turbulent shear stress predominates, and since the transition region is neglected in the model for the velocity profile, the values of $\tau_{Turb.}$ calculated from Eq. (1) and $\tau_{Lam.}$ calculated from Eq. (2) may be taken as each equal to the total shear stress at $y = \delta_L$. Thus a logical relationship between $\tau_{Turb.}$ and $\tau_{Lam.}$ would appear to be

$$\tau_{Turb.} = \tau_{Lam.} \text{ at } y = \delta_L$$

if $\tau_{Turb.}$ and $\tau_{Lam.}$ are computed as indicated above. In addition, if the von Karman mixing length formula

$$\ell = k \frac{\frac{du}{dy}}{\frac{d^2u}{dy^2}}$$

is used instead of the Prandtl mixing length formula, each of the shear stress assumptions will lead to another skin friction relation.

A study was therefore made to determine which of the assumptions and mixing length formula yielded a skin friction law which gave the best overall agreement between theory and experiment. It was found that Eq. (4) given by Donaldson, could best be adapted to the experimental results. The details of this analysis are contained in Appendix A.

described by a large amount of experimental velocity profile data. It was found that using this procedure and taking $\frac{r-1}{k^2}$ as constant resulted in a variation of n with Re_θ which is a good average of the available experimental data (references c, f, g, and h). This is shown in Figure 3. The value of the constant $\frac{r-1}{k^2}$ compatible with the n variation with Re_θ shown in Figure 3 is 20.0. This is only slightly different from the value of 22.5 given by Donaldson (reference e). Since in his analysis the n variation with Reynolds number was not considered and the Blasius (reference d) skin friction law was used to obtain the constant, it is to be expected that a slightly different constant would be obtained. The incompressible portion of the present analysis therefore represents an extension of the Donaldson analysis in that the n variation with Reynolds number is considered.

Compressible Turbulent Boundary Layers

8. Since for compressible flow, the temperature varies across the boundary layer, it is apparent that the assumption of constant shear stress through the laminar sublayer violates the stipulation that the velocity varies linearly with distance from the surface. It is assumed that this incompatibility does not introduce any serious errors in the skin friction results. The subsequent comparisons between theory and experiment tend to confirm this assumption.

9. The extension of the foregoing analysis to compressible flows is straightforward and the equations take the same form as those given in reference (e). If the value of the constant r obtained by the procedure described above is assumed to be the same for both incompressible and compressible flows with and without heat transfer, then Eq. (4) is valid for these cases if the density and viscosity contained in the Reynolds number are evaluated at the edge of the laminar sublayer. It is desirable, however, that the Reynolds number be expressed in terms of free-stream properties. This transformation is presented in reference (e) and in Appendix B where it is shown that the resulting equations necessary to determine local skin friction coefficients are as follows:

$$c_f = 2\left[20\ n\right]^{\frac{1-n}{1+n}} \left[\frac{1}{Re_\theta\left(\frac{\delta}{\theta}\right)}\right]^{\frac{2}{n+1}} \left[\frac{T_\infty}{T_L}\right]^{\frac{n-2\omega-1}{n+1}} \tag{7}$$

$$\frac{T_L}{T_\infty} = 1 + r.f.\frac{\gamma-1}{2} M_\infty^2\left[1-\left(\frac{u_L}{u_\infty}\right)^2\right] + \frac{T_w - T_s}{T_\infty}\left[1-\frac{u_L}{u_\infty}\right] \tag{8}$$

$$\frac{u_L}{u_\infty} = \left[\frac{20\ n}{Re_\theta\left(\frac{\delta}{\theta}\right)}\right]^{\frac{1}{n+1}} \times \left\{1 + r.f.\ \frac{\gamma - 1}{2} M_\infty^2 \left[1 - \left(\frac{u_L}{u_\infty}\right)^2\right] + \frac{T_w - T_e}{T_\infty}\left[1 - \frac{u_L}{u_\infty}\right]\right\}^{\frac{1.76}{n+1}} \quad (9)$$

10. Values of n for use in these equations are obtained from the curve of Figure 3. Using this single curve as a determining factor for n implies that n is uniquely related to Re_θ regardless of Mach number or heat transfer condition. Although the results shown in Figure 3 tend to justify this postulate, probably the Mach number and heat transfer influences on n are concealed by the insensitivity inherent in this coordinate system. A comparison between a plot of n versus Re_θ and n versus Re_δ indicates that some influence of Mach number and heat transfer is probably incorporated in both figures, but is appreciably less in the Re_θ plot. It is felt, therefore, that a more accurate determination of n may be obtained when Re_θ is used as the correlating factor.

11. Since Re_θ was chosen as the correlating factor for n and Eq. (7) requires the use of Re_δ, a means is therefore needed for converting given values of Re_θ to the equivalent Re_δ. The needed θ/δ values have been calculated using the definition for θ with Eq. (1) and the Crocco temperature distribution (reference e) for a series of Mach numbers up to 20, a wide range of heat transfer conditions, and n values of 5, 7, 9, and 11. These are tabulated in Table I. Also tabulated for the same range of variables are the values of δ^*/δ and H. It should be noted that the foregoing procedure for calculating these parameters ignores the laminar sublayer because the power profile is assumed to exist to the wall. While this procedure is not quite exact, it is felt that only small errors will result because by far the largest contributions to the integrals for δ^* and θ occur outside the laminar sublayer.

12. Using the present analysis, skin friction coefficients can be calculated if the Reynolds number is given in terms of either the total boundary layer thickness (Re_δ) or the boundary layer momentum thickness (Re_θ), or, as will be shown later, in terms of the distance from the leading edge. Since the dependence of θ/δ with Mach number and heat transfer is not considered in Donaldson's (reference e) analysis, the skin friction coefficient can be evaluated only if the value of Re_δ is known.

13. Whether or not the postulated uniqueness of n with Re_θ leads to serious errors may be checked by comparing the influence of n on c_f over a range of Mach numbers for a fixed value of Re_θ. A value of Re_θ of 8000 was selected for the check procedure,

and the n value was varied between 5.5 and 7.5 which encompasses the scatter of the experimental data at this point. It was found that the values of c_f over a range of Mach numbers up to 10 were no more than 6 percent above or below the curve drawn for the value of n theoretically associated with an Re_θ of 8000. On the basis of this check it was concluded that the skin friction values obtained from the present analysis are not particularly sensitive to the value of n associated with the Re_θ in question.

14. This result enables the approximate calculation of the variation of c_f/c_{f_i} as a function of Re_x. If c_f/c_{f_i} is not particularly sensitive to n, it may be assumed that for a given Mach number and heat transfer rate, the value of θ/δ along a plate is constant. This assumption is necessary to perform the integration indicated in Appendix C. Using this assumption, a relation between Re_δ and Re_x may be deduced. The details of this derivation are given in Appendix C, where it is shown that the resulting equation is

$$Re_\delta = Re_x^{\frac{n+1}{n+3}} \times \left\{ \left(\frac{\delta}{\theta}\right)^{n+1} \left(\frac{n+3}{n+1}\right)^{n+1} \left(\frac{1}{20n}\right)^{n-1} \left(\frac{T_\infty}{T_L}\right)^{n-2.52} \right\}^{\frac{1}{n+3}} \qquad (10)$$

It is not stipulated, however, that the value of (n) for use in equation (10) is a constant. Curves showing the variation of c_f/c_{f_i} as a function of Mach number for several constant values of wall temperature ratio and a constant value of Re_x of 10^7 (Figure 15) calculated using the equations of Appendix C are in good agreement with the empirical curves of Seiff (reference a). Results obtained using the equations of Appendix C should therefore suffice for most engineering applications.

15. The recent acquisition of detailed experimental data at hypersonic Mach numbers at both the Naval Ordnance Laboratory and the Applied Physics Laboratory (references c and f), both with and without steady state heat transfer, made it possible to examine not only the overall results of the theory but also the validity of the assumptions made and the use of constants drawn from incompressible flow results.

16. The first step is to examine the conditions at the edge of the laminar sublayer. This is necessary because the theory is focused on this point. For incompressible flows it has long been assumed that the value of $u_L^+ = y_L^+$ at the edge of the laminar sublayer (in the logarithmic velocity profile representation) is roughly a constant that lies between 11.0 and 12.0. The present analysis is not based on this assumption but is so constructed that a computation and check of the results obtained for this point may be made.

17. The theoretical variation of u_L^+ with Re_θ is compared with experimental data (references i and j) for incompressible flow in Figure 4. It is apparent that the accepted presumption that $u_L^+ - y_L^+$ is a constant is not far from true; however, the theory and experiment indicate that Reynolds number does influence the value of $u_L^+ - y_L^+$ slightly.

18. Figure 5 shows a comparison between the theoretical and experimental values (references c, f, and k) of $u_L^+ - y_L^+$ for compressible flow. For this comparison all values of $u_L^+ - y_L^+$ are based on wall properties. The theoretical curves associated with each set of experimental data were calculated such that they encompassed the experimental Mach number and Reynolds number range. Although the present analysis does not accurately predict the numerical values of $u_L^+ - y_L^+$ it does predict the proper trend of the data for both the heating and cooling cases.

19. In the formulation of this analysis, the incompressible skin friction law of Karman-Schoenherr has been used as a basis for the zero heat transfer case. Unfortunately, little experimental data are available which describe the influence of heat transfer on incompressible skin friction coefficients. The analysis can, however, be applied to this case and comparisons made with the few data that are available. The experimental results of reference (l), while not reported in sufficient detail to make an exact computation using the present analysis, may be used to show that it does predict qualitatively correct results. In using these experimental data for this comparison it is assumed that the ratio c_f/c_{f_i} can be used interchangeably with C_F/C_{F_i} and that little Reynolds number dependence on this ratio exists. Figure 6 shows both the predicted and experimental variation of c_f/c_{f_i} with wall temperature ratio for a constant value of Re_θ which represented a mean for the data of reference (l). The results shown in this figure demonstrate that the present analysis describes correctly the variation of c_f/c_{f_i} with increasing wall temperature ratio. Figure 7 shows the influence of heat transfer parameter on the values of c_f/c_{f_i} for several values of Mach number and a single value of Re_θ. It is apparent that cooling of the surface results in an increase in the skin friction coefficient, whereas heating has the opposite effect. That this result is consistent with the incompressible results shown in Figure 6 is evident from the results shown in Figure 8. This figure shows the variation of c_f/c_{f_i} with Mach number for several constant values of T_w/T_∞. The curves of constant T_w/T_∞ intercept the zero heat transfer curve at only one point. Each intercept occurs at the Mach number where $T_w/T_\infty = T_e/T_\infty$. A curve of the same appearance has been deduced by Seiff (reference m) from an empirical correlation of experimental data for Mach numbers up to about 5. A direct comparison between the results presented in Figure 8 and those reported in reference(m) is not valid because the curves of Figure 8 were computed for constant Re_θ and depend somewhat on this Reynolds number, whereas those of reference(m) are assumed to be independent of Reynolds number based on distance from the leading edge.

20. A comparison between specific values of experimental skin friction coefficients and the associated values predicted by the present analysis is shown in the following three figures. Figure 9 shows the variation of c_f/c_{f_i} with Mach number for zero heat transfer. All of the experimental data (references a, b, c, f, k, n, o, and p) shown were normalized to a constant Re_θ of 8000 and are either specifically for the case of zero heat transfer or were linearly extrapolated to the zero heat transfer condition. The scheme used for processing the heat transfer results is outlined in reference (c). Good agreement between theory and experiment is found for the entire range of Mach numbers for which experimental data are available. Figures 10 and 11 show comparisons between theoretical and experimental values of c_f/c_{f_i} plotted as a function of heat transfer parameter for those experimental data taken under conditions of steady state heat transfer (references c, f, and k). For each of the sets of data shown, the variation of Reynolds number with heat transfer rate, if any, was considered in the theoretical calculations. It is significant to note that the results shown for the data of reference (c) indicate little variation of skin friction ratio with increasing heat transfer. From the present analysis it appears that the increase in Reynolds number, which accompanied the increase in heat transfer rate, so influenced the results as to obviate any increase in skin friction ratio. In general, the agreement between theory and experiment is satisfactory for each of the sets of data shown.

CONCLUDING REMARKS

21. A theoretical investigation of compressible turbulent boundary layers with heat transfer has been conducted. This investigation is based on a simple flow model which is realistic for both the zero heat transfer and heat transfer conditions. The validity of the flow model assumed is demonstrated by comparisons between theoretical and experimental results. The theory is presented in such a fashion that values of skin friction may be calculated when either the Reynolds number based on boundary layer momentum thickness, total boundary layer thickness, or distance from the leading edge is given. Good agreement is demonstrated between theoretical and experimental values of skin friction coefficients, for both the zero and heat transfer conditions. It is shown that the predicted influence of heat transfer and Reynolds number on the properties at the edge of the laminar sublayer is consistent with the available experimental data for both incompressible and compressible flows. It is anticipated that, with the acquisition of additional data covering a broader range of conditions, improvements will be made in both the functional nature and accuracy of the analysis.

REFERENCES

(a) Rubesin, M. W., Maydew, R. C., and Varga, S. A., "An Analytical and Experimental Investigation of the Skin Friction of the Boundary Layer on a Flat Plate at Supersonic Speeds," NACA TN 2305, February 1951.

(b) Chapman, Dean R. and Kester, Robert H., "Measurements of Turbulent Skin Friction on Cylinders in Axial Flow at Subsonic and Supersonic Velocities." Paper presented at 21st Annual Meeting, I.A.S., New York, N.Y. January 26-29, 1953 (Preprint No. 391).

(c) Lobb, R. K., Winkler, E. M., and Persh, Jerome, "Experimental Investigation of Turbulent Boundary Layers in Hypersonic Flow," NAVORD Report 3880, February 1955.

(d) Prandtl, L., "The Mechanics of Viscous Fluids," Vol. III, Aerodynamic Theory, W. F. Durand, editor, 1943.

(e) Donaldson, C. Du P., "Skin Friction and Heat Transfer through Turbulent Boundary Layers for Incompressible Flows and Compressible Flows" (presented at the Heat Transfer and Fluid Mechanics Institute Meeting in Los Angeles, Calif., June 1952).

(f) Hill, F. K., "Boundary-Layer Measurements in Hypersonic Flow" (to be published in the Journal of Aeronautical Sciences).

(g) Ross, Donald, "A Study of Incompressible Turbulent Boundary Layers," Technical Memorandum, ONR Project NR 062-139-1, Ordnance Research Laboratory, The Pennsylvania State College, School of Engineering, State College, Pennsylvania, June 1953.

(h) Wilson, R. E., "Turbulent Boundary Layer Characteristics at Supersonic Speeds --Theory and Experiment," J. Aeronaut. Sci., Vol. 17, No. 9, p. 585, September 1950.

(i) Ross, Donald, "Turbulent Flow in Smooth Pipes --A Reanalysis of Nikuradses' Experiments," Ordnance Research Laboratory, The Pennsylvania State College, State College, Pennsylvania, Serial No. NOrd 7958-246, September 1952.

(j) Laufer, John, "Investigation of Turbulent Flow in a Two-Dimensional Channel," NACA Report 1053, 1951.

(k) Monaghan, R. J. and Cooke, J. R., "The Measurement of Heat Transfer and Skin Friction at Supersonic Speeds. Part III - Measurements of Overall Heat Transfer and of the Associated Boundary Layers on a Flat Plate at M = 2.43," R. A. E. Tech. Note No. AERO 2127, Dec. 1951.

(l) Humble, Leroy V., Lowdermilk, Warren H., and Desmon, Leland G., "Measurements of Average Heat Transfer and Friction Coefficients for Subsonic Flow of Air in Smooth Tubes at High Surface and Fluid Temperatures," NACA Report 1020, 1951.

(m) Seiff, Alvin, "Examination of the Existing Data on the Heat Transfer of Turbulent Boundary Layers at Supersonic Speeds form the Viewpoint of Reynolds Analogy," NACA TN 3284, August 1954.

(n) Coles, Donald, "Measurements in the Boundary Layer on a Smooth Flat Plate in Supersonic Flow," Thesis, California Institute of Technology, May 1953.

(o) Brinich, Paul F. and Diaconis, Nick S., "Boundary Layer Development and Skin Friction at a Mach Number 3.05," NACA TN 2742, 1952.

(p) Korgeki, R. H., "Transition Studies and Skin Friction Measurements on an Insulated Flat Plate at a Hypersonic Mach Number," California Institute of Technology, Guggenheim Aeronautical Laboratory, Hypersonic Wind Tunnel, Pasadena, California, Memorandum No. 17, July 1954.

(q) Weiler, T. E. and Hartwig, W. H., "The Direct Measurement of Local Skin Friction Coefficient," Report CF-174,, DRL-295, Defense Research Laboratory, University of Texas, Austin, Texas, September 1952.

APPENDIX A

General Relations for the Local Skin Friction Coefficient

1. The equation of motion to be satisfied by a boundary layer flowing on a flat plate in the absence of a pressure gradient is:

$$u \frac{du}{dx} + v \frac{du}{dy} = \frac{1}{\rho} \frac{d\tau}{dy} = \frac{1}{\rho} \frac{d}{dy} \left[\mu \frac{du}{dy} + \rho \ell^2 \left(\frac{du}{dy} \right)^2 \right] \qquad \text{(A1)}$$

The total shear stress at any point in the boundary layer is

$$\tau_{Lam.} + \tau_{Turb.} = \mu \frac{du}{dy} + \rho \ell^2 \left(\frac{du}{dy} \right)^2 \qquad \text{(A2)}$$

Donaldson (reference e) assumed that the ratio of the total stress to the laminar stress at the edge of the laminar sublayer is a constant,

$$\frac{\tau_{Lam.} + \tau_{Turb.}}{\tau_{Lam.}} = r = \text{constant} \quad \text{at } y = \delta_L \qquad \text{(A3)}$$

Using this assumption, and evaluating Eq. A2 at $y = \delta_L$ by using,

$$\frac{du}{dy} = \frac{u_\infty \delta_L^{\frac{1-n}{n}}}{n\, \delta^{1/n}} \qquad \text{(A4)}$$

which is obtained from the power profile (Eq. 1), it can be shown that the thickness ratio of the laminar sublayer is

$$\frac{\delta_L}{\delta} = \left[\frac{n(r-1)\, \delta_L^2}{\ell^2 \; Re_\delta} \right]^{\frac{n}{n+1}} \qquad \text{(A5)}$$

2. It may also be logically assumed that at $y = \delta_L$, the laminar shear stress is equal to the turbulent shear stress

$$\tau_{Lam.} = \tau_{Turb.} \quad \text{at } y = \delta_L$$

Evaluating $\tau_{Turb.}$ using Eq. 1 and $\tau_{Lam.}$ using Eq. 2 yields the following expression for the thickness ratio of the laminar sublayer

$$\frac{\delta_L}{\delta} = \left[\frac{n^2\,\delta^2}{\ell^2}\;\frac{1}{Re_\delta}\right]^{\frac{n}{1-n}} \qquad \text{(A6)}$$

Equations (A5) and (A6) necessarily contain the so far undetermined mixing length "ℓ" for which either the Prandtl mixing length law

$$\ell = k\,y \qquad \text{(A7)}$$

or the von Karman mixing length law

$$\ell = k\,\frac{\frac{du}{dy}}{\frac{d^2u}{dy^2}} \qquad \text{(A8)}$$

may be used.

3. It is evident therefore, that the assumptions used to obtain equations (A5) and (A6) together with the mixing length laws given in equations (A7) and (A8) will yield four equations for the thickness ratio of the laminar sublayer. These are tabulated below:

Assumption	Mixing length law	Laminar sublayer thickness ratio
Equation (A5)	Prandtl (Eq. A7)	$\frac{\delta_L}{\delta} = \left[\frac{n(r-1)}{k^2\,Re_\delta}\right]^{\frac{n}{n+1}}$
	von Karman (Eq. A8)	$\frac{\delta_L}{\delta} = \left[\frac{n(r-1)}{k^2\,Re_\delta}\right]^{\frac{n}{n+1}}\left[\frac{1-n}{n}\right]^{\frac{2n}{n+1}}$
Equation (A6)	Prandtl (Eq. A7)	$\frac{\delta_L}{\delta} = \left[\frac{n^2}{k^2\,Re_\delta}\right]^{\frac{n}{n+1}}$
	von Karman (Eq. A8)	$\frac{\delta_L}{\delta} = \left[\frac{n^2}{k^2\,Re_\delta}\right]^{\frac{n}{n+1}}\left[\frac{1-n}{n}\right]^{\frac{2n}{n+1}}$

The local skin friction coefficient for incompressible flow may be calculated using the substitutions

$$\tau_w = \frac{u_L}{\delta_L}$$

$$\frac{u_L}{U_\infty} = \left(\frac{\delta_L}{\delta}\right)^{\frac{1}{n}}$$

and

$$c_f = \frac{2\,\tau_w}{\rho_\infty U_\infty^{\,2}}$$

together with each of the equations for the laminar sublayer thickness ratio. These are tabulated below.

Assumption	Mixing length law	Local skin friction coefficient law
Equation (A5)	Prandtl (Eq. A7)	$c_{f_i} = 2\left[\frac{n(r-1)}{k^2}\right]^{\frac{1-n}{1+n}}\left[\frac{1}{Re_\delta}\right]^{\frac{2}{n+1}}$ (A9)
	von Karman (Eq. A8)	$c_{f_i} = 2\left[\frac{n(r-1)}{k^2}\right]^{\frac{1-n}{1+n}}\left[\frac{1}{Re_\delta}\right]^{\frac{2}{n+1}}\left[\frac{1-n}{n}\right]^{\frac{2(1-n)}{1+n}}$ (A10)
Equation (A6)	Prandtl (Eq. A7)	$c_{f_i} = 2\left[\frac{n^2}{k^2}\right]^{\frac{1-n}{1+n}}\left[\frac{1}{Re_\delta}\right]^{\frac{2}{n+1}}$ (A11)
	von Karman (Eq. A8)	$c_{f_i} = 2\left[\frac{n^2}{k^2}\right]^{\frac{1-n}{1+n}}\left[\frac{1}{Re_\delta}\right]^{\frac{2}{n+1}}\left[\frac{1-n}{n}\right]^{\frac{2(1-n)}{1+n}}$ (A12)

APPENDIX B

Derivation of Local Skin Friction Coefficient Law for Compressible Turbulent Boundary Layers

1. It has been shown that equation (4) was the most suitable for incompressible turbulent boundary layers. This law is given as

$$c_{f_i} = 2\left[20n\right]^{\frac{1-n}{1+n}}\left[\frac{1}{Re_\delta}\right]^{\frac{2}{n+1}} \qquad (4)$$

To extend this relation to compressible flows the property values (density and viscosity) need be evaluated at the edge of the laminar sublayer. Equation (4) may be written in the form

$$\frac{\tau_w}{\rho_\infty u_\infty^2} = \left[20n\right]^{\frac{1-n}{1+n}}\left[\frac{\mu_\infty}{\rho_\infty u_\infty \delta}\right]^{\frac{2}{n+1}}\left[\frac{\nu_L}{\nu_\infty}\right]^{\frac{2}{n+1}}\left[\frac{\rho_L}{\rho_\infty}\right] \qquad (B1)$$

using the following substitutions

$$\frac{\rho_L}{\rho_\infty} = \frac{T_\infty}{T_L}$$

and

$$\frac{\mu_L}{\mu_\infty} = \left[\frac{T_L}{T_\infty}\right]^{\omega}$$

in equation (B1), yields the following relationship:

$$c_f = 2\left[20n\right]^{\frac{1-n}{1+n}}\left[\frac{1}{Re_\delta}\right]^{\frac{2}{n+1}}\left[\frac{T_\infty}{T_L}\right]^{\frac{n-2\omega-1}{n+1}} \qquad (B2)$$

2. To evaluate $\frac{T_\infty}{T_L}$ it will be assumed that the Crocco quadratic form for the temperature distribution given as

$$T = A + B\left[\frac{u}{u_\infty}\right] + C\left[\frac{u}{u_\infty}\right]^2 \qquad (B3)$$

is valid By evaluating equation (B3) with the usual boundary conditions, the following equation results

$$\frac{T_L}{T_\infty} = \frac{T_w}{T_\infty} - \left[\frac{T_w - T_e}{T_\infty}\right]\left[\frac{u_L}{u_\infty}\right] - \left[\frac{T_e - T_\infty}{T_\infty}\right]\left[\frac{u_L}{u_\infty}\right]^2 \qquad \text{(B4)}$$

3. Equation (B4) may also be written as

$$\frac{T_L}{T_\infty} = 1 + r.f. \frac{\gamma-1}{2} M_\infty^2 \left[1 - \left(\frac{u_L}{u_\infty}\right)^2\right] + \frac{T_w - T_e}{T_\infty}\left[1 - \frac{u_L}{u_\infty}\right] \qquad \text{(B5)}$$

with the velocity ratio at the edge of the laminar sublayer given as

$$\frac{u_L}{u_\infty} = \left|\frac{20n}{Re_\delta}\right|^{\frac{1}{n+1}} \left\{1 + r.f. \frac{\gamma-1}{2} M_\infty^2 \left[1 - \left(\frac{u_L}{u_\infty}\right)^2\right] + \frac{T_w - T_e}{T_\infty}\left[1 - \frac{u_L}{u_\infty}\right]\right\}^{\frac{\omega+1}{n+1}} \qquad \text{(B6)}$$

4. For all calculations using equations (B2), (B5) and (B6) ω has been taken as 0.76 and the value of r.f. as 0.896.

APPENDIX C

Derivation of Local and Average Skin Friction Coefficient Laws Based on Re_x

1. For incompressible flow the momentum equation for the boundary layer in the absence of a pressure gradient is

$$\frac{d\theta}{dx} = \frac{C_f}{2} \qquad (C1)$$

or

$$\frac{dRe_\theta}{dRe_x} = \frac{C_f}{2} \qquad (C2)$$

The following relation results when the right hand side of equation (4) is inserted into equation (C2);

$$\frac{dRe_\theta}{dRe_x} = \left[20n\right]^{\frac{1-n}{1+n}} \left[\frac{1}{Re_\theta}\right]^{\frac{2}{n+1}} \left[\frac{n}{(n+1)(n+2)}\right]^{\frac{2}{n+1}} \qquad (C3)$$

and the substitution $\frac{\delta}{\theta} = \frac{(n+1)(n+2)}{n}$ is used.

Equation (C3) can be integrated by assuming that n is a constant along a given plate (or $\frac{\theta}{\delta}$ is constant). Whether or not this is a valid assumption will be verified by a comparison between the von Karman incompressible mean skin friction law and the derived relationship. Integrating equation (C3) yields

$$(Re_\theta)^{\frac{n+3}{n+1}} = \frac{n+3}{n+1} \left[\frac{1}{20n}\right]^{\frac{n-1}{n+1}} \left[\frac{n}{(n+1)(n+2)}\right]^{\frac{2}{n+1}} Re_x \qquad (C4)$$

and since

$$\frac{C_{Fi}}{2} = \frac{Re_\theta}{Re_x} \qquad (C5)$$

equation (C4) can be manipulated to yield

$$\frac{C_{Fi}}{2} = \left\{ \left[\frac{n+3}{n+1}\right] \left[\frac{1}{20n}\right]^{\frac{n-1}{n+1}} \left[\frac{n}{(n+1)(n+2)}\right]^{\frac{2}{n+1}} \right\}^{\frac{n+1}{n+3}} \left[\frac{1}{Re_x}\right]^{\frac{2}{n+3}} \tag{C6}$$

A comparison between the values of C_{Fi} obtained from equation (C6) (using the n values associated with the Re_θ values of figure 3 and equation (C4)) and the values of C_{Fi} from the von Karman mean skin friction equation for incompressible flow

$$\frac{0.242}{\sqrt{C_{Fi}}} = \operatorname{Log}_{10}\left[C_{Fi}\ Re_x\right] \tag{C7}$$

indicated that over the Reynolds number (Re_x) range from 0.5×10^6 to 60×10^6 the agreement between C_{Fi} values is within 4 percent. This result means that at least for incompressible flow the assumption that n is a constant along a plate can only lead to small errors in the estimation of skin friction values.

Using this information, the incompressible law for local skin friction coefficients on a Re_x basis may then be derived. The momentum equation can be written as

$$\frac{d\delta}{dx} = \frac{\delta}{2\theta} c_f \tag{C8}$$

Substituting equation (4) yields

$$\frac{d\delta}{dx} = \frac{\delta}{2\theta}\left[20n\right]^{\frac{1-n}{1+n}} \left[\frac{1}{Re_\theta}\right]^{\frac{2}{n+1}} \left[\frac{n}{(n+1)(n+2)}\right]^{\frac{2}{n+1}} \tag{C9}$$

which may be integrated to yield the following relation

$$\frac{Re_\delta}{Re_x} = \left[\frac{n+3}{n+1}\left(\frac{\delta}{\theta}\right)\right]^{\frac{n+1}{n+3}} \cdot \left[\frac{1}{20n}\right]^{\frac{n-1}{n+3}} \left[\frac{1}{Re_x}\right]^{\frac{2}{n+3}} \tag{C10}$$

By inserting equation (C10) into equation (C3) the following local skin friction law results

$$\frac{C_{fi}}{2} = \left[\frac{1}{20n}\right]^{\frac{n-1}{n+3}} \left[\frac{n+1}{n+3}\left(\frac{\theta}{\delta}\right)\right]^{\frac{2}{n+3}} \left[\frac{1}{Re_x}\right]^{\frac{2}{n+3}} \tag{C11}$$

or

$$\frac{C_{fi}}{2} = \left[\frac{1}{20n}\right]^{\frac{n-1}{n+3}} \left[\frac{n}{(n+2)(n+3)}\right]^{\frac{2}{n+3}} \left[\frac{1}{Re_x}\right]^{\frac{2}{n+3}} \tag{C12}$$

2. For compressible flow the extension of the foregoing expressions for the mean and local skin friction coefficients to compressible flows necessitates the use of an additional approximation the accuracy of which is checked with the available experimental data.

The local skin friction law (equation B2)

$$\frac{C_f}{2} = \left[\frac{1}{20n}\right]^{\frac{n-1}{n+1}} \left[\frac{1}{Re_\delta}\right]^{\frac{2}{n+1}} \left[\frac{T_\infty}{T_L}\right]^{\frac{n-2.52}{n+1}} \tag{B2}$$

embodies the term $\left(\frac{T_\infty}{T_L}\right)$ which cannot be a predetermined constant because it depends on Reynolds number as can be seen in the following equations:

$$\frac{T_L}{T_\infty} = 1 + r.f. \frac{\gamma-1}{2} M_\infty^2 \left[1 - \left(\frac{u_L}{u_\infty}\right)^2\right] + \frac{T_w - T_e}{T_\infty}\left[1 - \frac{u_L}{u_\infty}\right] \tag{C13}$$

where

$$\frac{u_L}{u_\infty} = \left[\frac{20n}{Re_\delta}\right]^{\frac{1}{n+1}} \left[\frac{T_L}{T_\infty}\right]^{\frac{1.76}{n+1}} \qquad \text{(B6) or (C14)}$$

However, if $\frac{T_\infty}{T_L}$ is assumed to be a constant that is associated with an average value of Reynolds number, the results that are obtained may be of sufficient accuracy for most applications. This is a logical step because for a given Mach number and heat transfer rate $\frac{u_L}{u_\infty}$ is not seriously dependent on Re_δ or Re_x. Using this assumption, the following relations may be derived from an integration of equation (B2).

$$\frac{C_F}{2} = \left\{ \left[\frac{n+3}{n+1}\right]^{n+1} \left[\frac{1}{20n}\right]^{n-1} \left[\frac{\theta}{\delta}\right]^{2} \left[\frac{T_\infty}{T_L}\right]^{n-2.52} \left[\frac{1}{\overline{Re}_x}\right]^{2} \right\}^{\frac{1}{n+3}} \quad \text{(C15)}$$

and

$$Re_\delta = \left[\overline{Re}_x\right]^{\frac{n+1}{n+3}} \left[\left(\frac{\delta}{\theta}\right)^{n+1} \left(\frac{n+3}{n+1}\right)^{n+1} \left(\frac{1}{20n}\right)^{n-1} \left(\frac{T_\infty}{T_L}\right)^{n-2.52} \right]^{\frac{1}{n+3}} \quad \text{(C16)}$$

where $\overline{Re}_x$ is given by

$$\overline{Re}_x = \tfrac{1}{2}\, Re_x \text{ (maximum)}$$

To determine local skin friction coefficients with the knowlege of only values of Re_x it is necessary to have available the variation of n with Re_x and Re_δ for use in equation (C16). A calculation of the variation of n with Re_x and Re_δ has been carried out for the zero heat transfer case and the results are plotted in figures 12 and 13 respectively. These calculations were made using the results tabulated in Table I, figure 3, and equations (C13) and C14). Curves similar to those shown in figures 12 and 13 may be prepared for different heat transfer rates by the same method.

Using the data plotted in figures 12 and 13 the procedure for calculating C_f as a function of Re_x is as follows:

1. Determine the maximum value of Re_x to be encounted for a given problem. The selection of this value determines n, Re_δ, and Re_x.

2. Solve equation (C16) for $\frac{T_\infty}{T_L}$.

3. Insert the values of $\frac{T_\infty}{T_L}$, n, and Re_δ in equation (B2) and solve for C_f.

By a similar procedure equation (C15) may be used to calculate mean skin friction coefficients.

As a check on the approximate analysis described above, the variation of c_f/c_{fi} with Mach number has been carried out for three values of $\overline{Re}_x$ sufficient to encompass the Re_x range of the available experimental data. Figure 14 shows the results of these calculations compared to the available experimental data. The good agreement between theory and experiment tends to justify the approximations made in the preceding analysis.

Figure 15 shows the variation of the skin friction ratio with Mach number for a number of constant values of wall to free stream temperature ratio and a constant value of Re_x of 10^7. The similarity between curves of this figure and the results plotted in figure 8 is apparent. However, differences in the curve shapes and corresponding values of the skin friction ratio can be seen by careful examination.

TABLE I

VARIATION OF DISPLACEMENT THICKNESS RATIO, $\frac{\delta^*}{\delta}$, MOMENTUM THICKNESS RATIO, $\frac{\theta}{\delta}$, AND BOUNDARY LAYER SHAPE PARAMETER WITH MACH NUMBER, M, AND HEAT TRANSFER PARAMETER, $\frac{T_w - T_e}{T_\infty}$, FOR A VELOCITY PROFILE EXPONENT, n, OF 5.0

n	$\frac{T_w - T_e}{T_\infty}$	M_∞	$\frac{\delta^*}{\delta}$	$\frac{\theta}{\delta}$	H
5.0	0	0	0.10741	0.11882	1.40088
		2.0	0.28470	0.09266	3.07252
		4.0	0.46891	0.05842	7.99213
		6.0	0.60324	0.03746	16.10281
		8.0	0.69592	0.02543	27.36533
		10.0	0.75980	0.01816	41.83921
		12.0	0.80518	0.01354	59.46824
		14.0	0.83844	0.01044	80.30651
		16.0	0.86347	0.00828	104.28746
		18.0	0.88275	0.00671	132.56483
		20.0	0.89787	0.00555	161.78378
5.0	2.0	0	0.33149	0.08204	4.04071
		2.0	0.39674	0.06996	5.67038
		4.0	0.52041	0.04937	10.54081
		6.0	0.62891	0.03378	18.61753
		8.0	0.70932	0.02374	29.87784
		10.0	0.76737	0.01732	44.30718
		12.0	0.80976	0.01306	61.91131
		14.0	0.84137	0.01017	82.73353
		16.0	0.86543	0.00811	106.70777
		18.0	0.88410	0.00661	133.73189
		20.0	0.89884	0.00547	164.31444
5.0	4.0	0	0.42494	0.06438	6.60968
		2.0	0.46907	0.05706	8.21829
		4.0	0.56127	0.04297	13.06260
		6.0	0.65068	0.03081	21.11652
		8.0	0.72130	0.02229	32.35980
		10.0	0.77437	0.01655	46.79184
		12.0	0.81409	0.01264	64.40668
		14.0	0.84417	0.00991	85.18668
		16.0	0.86732	0.00794	109.23174
		18.0	0.88542	0.00649	136.42627
		20.0	0.89978	0.00540	166.62963
5.0	6.0	0	0.48867	0.05335	9.12608
		2.0	0.52137	0.04858	10.73944
		4.0	0.59392	0.03818	15.56780
		6.0	0.66930	0.02836	23.60014
		8.0	0.73210	0.02101	34.84531
		10.0	0.78087	0.01583	49.28814
		12.0	0.81818	0.01224	66.84641
		14.0	0.84685	0.00967	87.58014
		16.0	0.86914	0.00779	111.56611
		18.0	0.88670	0.00639	138.74389
		20.0	0.90070	0.00533	168.96487
5.0	8.0	0	0.53607	0.04606	11.63411
		2.0	0.56165	0.04249	13.26140
		4.0	0.62083	0.03436	18.05701
		6.0	0.68561	0.02629	26.07036
		8.0	0.74190	0.01989	37.30018
		10.0	0.78692	0.01522	51.70171
		12.0	0.82206	0.01186	69.31703
		14.0	0.84943	0.00943	90.07423
		16.0	0.87091	0.00763	114.14158
		18.0	0.88794	0.00629	141.16057
		20.0	0.90160	0.00526	171.40684
5.0	10.0	0	0.57328	0.04068	14.18818
		2.0	0.59399	0.03776	15.73093
		4.0	0.64352	0.03133	20.53948
		6.0	0.70001	0.02451	28.58977
		8.0	0.75068	0.01888	39.77228
		10.0	0.79250	0.01463	54.17638
		12.0	0.82574	0.01150	71.80000
		14.0	0.85190	0.00920	92.59783
		16.0	0.87261	0.00749	116.50200
		18.0	0.88918	0.00619	143.65109
		20.0	0.90248	0.00519	173.89518

VARIATION OF DISPLACEMENT THICKNESS RATIO, $\frac{\delta^*}{\delta}$, MOMENTUM THICKNESS RATIO, $\frac{\theta}{\delta}$, AND BOUNDARY LAYER SHAPE PARAMETER WITH MACH NUMBER, M, AND HEAT TRANSFER PARAMETER, $\frac{T_w - T_e}{T_\infty}$, FOR A VELOCITY PROFILE EXPONENT, n, OF 7.0

n	$\frac{T_w - T_c}{T_\infty}$	M_∞	$\frac{\delta^*}{\delta}$	$\frac{\theta}{\delta}$	H
7.0	0	0	0.12669	0.09781	1.29574
		2.0	0.22779	0.07861	2.89785
		4.0	0.39999	0.05327	7.65257
		6.0	0.53914	0.03479	15.49583
		8.0	0.63887	0.02416	26.44434
		10.0	0.71002	0.01756	40.43280
		12.0	0.76187	0.01324	57.54532
		14.0	0.80058	0.01028	77.80369
		16.0	0.83012	0.00821	101.10840
		18.0	0.85310	0.00670	127.32836
		20.0	0.87130	0.00556	1[illegible] 70063
7.0	2.0	0	0.26818	0.07124	3.76474
		2.0	0.33018	0.06181	6.34218
		4.0	0.43278	0.04503	10.05552
		6.0	0.56600	0.03168	17.88310
		8.0	0.65344	0.02268	28.80987
		10.0	0.71851	0.01678	42.81883
		12.0	0.76712	0.01281	59.86290
		14.0	0.80394	0.01006	80.07968
		16.0	[illegible]	0.00806	103.27543
		18.0	0.85471	0.00659	129.69651
		20.0	0.87245	0.00549	158.92532
7.0	4.0	0	0.35032	0.05763	6.18081
		2.0	0.40004	0.05164	7.74503
		4.0	0.49424	0.03971	12.44883
		6.0	0.58902	0.02909	20.24781
		8.0	0.66657	0.02140	31.14083
		10.0	[illegible]	0.01610	45.11801
		12.0	0.77300	0.01241	62.21563
		14.0	0.80725	0.00979	82.48170
		16.0	0.83485	0.00789	105.79214
		18.0	0.85628	0.00648	132.14506
		20.0	0.87339	0.00541	161.47674
7.0	6.0	0	0.41890	0.04888	8.56997
		2.0	0.48231	0.04464	10.13817
		4.0	0.52502	0.03565	14.81068
		6.0	0.60905	0.02694	22.60950
		8.0	0.67850	0.02028	33.50617
		10.0	0.73373	0.01548	47.40867
		12.0	0.77679	0.01203	64.57190
		14.0	0.81036	0.00957	84.68130
		16.0	0.83679	0.00778	107.83505
		18.0	0.85780	0.00639	134.34100
		20.0	0.87488	0.00534	163.80180
7.0	8.0	0	0.46686	0.04265	10.94728
		2.0	0.49355	0.03947	12.50570
		4.0	0.55653	0.03230	17.23910
		6.0	0.62671	0.02511	24.98818
		8.0	0.68727	0.01983	34.87709
		10.0	0.74060	0.01488	49.83840
		12.0	0.78126	0.01168	66.89312
		14.0	0.81339	0.00934	87.08779
		16.0	0.83888	0.00761	110.33653
		18.0	0.85929	0.00629	136.61387
		20.0	0.87577	0.00527	166.19596
7.0	10.0	0	0.50593	0.03795	13.31469
		2.0	0.52729	0.03546	14.87068
		4.0	0.58048	0.02972	19.53538
		6.0	0.64243	0.02353	27.30132
		8.0	0.69938	0.01832	38.17686
		10.0	0.74704	0.01432	52.18480
		12.0	0.78532	0.01135	69.20705
		14.0	0.81628	0.00913	89.40684
		16.0	0.84090	0.00747	112.57026
		18.0	0.86073	0.00620	138.85358
		20.0	0.87683	0.00521	168.29175

TABLE I (CONTINUED)

VARIATION OF DISPLACEMENT THICKNESS RATIO, $\frac{\delta^*}{\delta}$, MOMENTUM THICKNESS RATIO, $\frac{\theta}{\delta}$, AND BOUNDARY LAYER SHAPE PARAMETER WITH MACH NUMBER, M, AND HEAT TRANSFER PARAMETER, $\frac{T_w - T_e}{T_\infty}$, FOR A VELOCITY PROFILE EXPONENT, n, OF 9.0

n	$\frac{T_w - T_e}{T_\infty}$	M_∞	$\frac{\delta^*}{\delta}$	$\frac{\theta}{\delta}$	H
9.0	0	0	0.10083	0.08100	1.23071
		2.0	0.19941	0.06803	2.79877
		4.0	0.36160	0.04714	7.45863
		6.0	0.46998	0.03331	15.10240
		8.0	0.59384	0.02309	25.91828
		10.0	0.66911	0.01686	39.88848
		12.0	0.72884	0.01288	56.47814
		14.0	0.76830	0.01007	76.18503
		16.0	0.80132	0.00808	99.17079
		18.0	0.82784	0.00663	124.95406
		20.0	0.84790	0.00551	153.88388
9.0	2.0	0	0.28870	0.06863	3.60830
		2.0	0.38390	0.05807	6.15828
		4.0	0.40277	0.04117	9.78308
		6.0	0.51716	0.02961	17.46707
		8.0	0.60651	0.02138	28.19741
		10.0	0.67021	0.01617	41.94187
		12.0	0.73127	0.01248	58.73898
		14.0	0.77307	0.00983	78.84527
		16.0	0.80390	0.00792	101.80283
		18.0	0.82905	0.00658	127.18288
		20.0	0.84921	0.00544	156.10294
9.0	4.0	0	0.30780	0.05184	5.93943
		2.0	0.35034	0.04685	7.47708
		4.0	0.44377	0.03671	12.08938
		6.0	0.54077	0.02736	19.76608
		8.0	0.62336	0.02048	30.47092
		10.0	0.68670	0.01583	44.21764
		12.0	0.73670	0.01207	61.03583
		14.0	0.77560	0.00960	80.80208
		16.0	0.80638	0.00778	103.65039
		18.0	0.83062	0.00641	129.60996
		20.0	0.85049	0.00537	158.37989
9.0	6.0	0	0.36826	0.04462	8.38418
		2.0	0.40137	0.04108	9.76547
		4.0	0.47772	0.03321	14.38432
		6.0	0.56148	0.02547	22.04584
		8.0	0.63500	0.01939	32.74884
		10.0	0.69463	0.01484	46.49204
		12.0	0.74188	0.01173	63.24808
		14.0	0.77917	0.00937	83.15902
		16.0	0.80879	0.00763	105.72549
		18.0	0.83284	0.00631	131.93344
		20.0	0.85175	0.00529	161.02079
9.0	8.0	0	0.41840	0.03937	10.88378
		2.0	0.44839	0.03660	12.00743
		4.0	0.50880	0.03037	16.87764
		6.0	0.57989	0.02384	24.32464
		8.0	0.64660	0.01844	35.02708
		10.0	0.70207	0.01440	48.75894
		12.0	0.74678	0.01139	65.56629
		14.0	0.78281	0.00917	85.33261
		16.0	0.81113	0.00750	108.14667
		18.0	0.83432	0.00622	134.11976
		20.0	0.85298	0.00523	163.40996
9.0	10.0	0	0.45309	0.03534	12.84380
		2.0	0.47639	0.03315	14.37104
		4.0	0.53172	0.02803	18.95480
		6.0	0.59838	0.02242	26.60135
		8.0	0.65728	0.01763	37.28304
		10.0	0.70907	0.01390	51.01439
		12.0	0.75148	0.01108	67.82491
		14.0	0.78573	0.00897	87.59197
		16.0	0.81340	0.00736	110.31630
		18.0	0.83595	0.00611	136.36213
		20.0	0.85417	0.00517	165.32244

VARIATION OF DISPLACEMENT THICKNESS RATIO, $\frac{\delta^*}{\delta}$, MOMENTUM THICKNESS RATIO, $\frac{\theta}{\delta}$, AND BOUNDARY LAYER SHAPE PARAMETER WITH MACH NUMBER, M, AND HEAT TRANSFER PARAMETER, $\frac{T_w - T_e}{T_\infty}$, FOR A VELOCITY PROFILE EXPONENT, n, OF 11.0

n	$\frac{T_w - T_e}{T_\infty}$	M_∞	$\frac{\delta^*}{\delta}$	$\frac{\theta}{\delta}$	H
11.0	0	0	0.08371	0.07040	1.18892
		2.0	0.18340	0.05994	2.73273
		4.0	0.31456	0.04290	7.33333
		6.0	0.45036	0.03019	14.98358
		8.0	0.55537	0.02171	25.59246
		10.0	0.63437	0.01618	39.20690
		12.0	0.69416	0.01244	55.80306
		14.0	0.74006	0.00981	75.44343
		16.0	0.77584	0.00792	97.98455
		18.0	0.80416	0.00650	123.72306
		20.0	0.82665	0.00542	152.56456
11.0	2.0	0	0.19588	0.05877	3.30108
		2.0	0.24951	0.04961	5.02933
		4.0	0.38380	0.03789	9.00148
		6.0	0.47759	0.02777	17.19842
		8.0	0.57105	0.02084	27.80428
		10.0	0.64391	0.01554	41.43801
		12.0	0.70028	0.01207	58.01988
		14.0	0.74411	0.00959	77.59134
		16.0	0.77864	[illegible]	100.53805
		18.0	0.80614	[illegible]	[illegible]
		20.0	0.82829	0.00540	153.38889
11.0	4.0	0	0.27171	0.04700	5.78063
		2.0	0.31347	0.04270	7.30311
		4.0	0.40302	0.03106	11.85849
		6.0	0.50138	0.02580	19.43411
		8.0	0.58535	0.01949	30.03592
		10.0	0.65283	0.01496	43.63836
		12.0	0.70604	[illegible]	60.23881
		14.0	0.74801	0.00936	79.91453
		16.0	0.78134	0.00762	102.53281
		18.0	0.80806	0.00631	128.06656
		20.0	0.82970	0.00529	156.84310
11.0	6.0	0	0.33943	0.04095	8.04390
		2.0	0.36180	0.03784	9.50131
		4.0	0.43758	0.03101	14.11188
		6.0	0.53242	0.02410	21.67838
		8.0	0.59846	0.01854	32.20155
		10.0	0.66119	0.01441	45.88480
		12.0	0.71158	0.01139	62.47388
		14.0	0.75178	0.00916	82.07424
		16.0	0.78396	0.00749	104.67290
		18.0	0.80994	0.00622	130.20900
		20.0	0.83107	0.00523	158.91013
11.0	8.0	0	0.37540	0.03646	10.29022
		2.0	0.40208	0.03403	11.61604
		4.0	0.46633	0.02852	16.34993
		6.0	0.54122	0.02264	23.90459
		8.0	0.61052	0.01770	34.49153
		10.0	0.66904	0.01392	48.08036
		12.0	0.71680	0.01110	64.57858
		14.0	0.75534	0.00898	84.30804
		16.0	0.78650	0.00738	106.88141
		18.0	0.81178	0.00613	132.41067
		20.0	0.83241	0.00517	161.00580
11.0	10.0	0	0.41330	0.03297	12.53584
		2.0	0.43581	0.03102	14.04800
		4.0	0.49137	0.02643	18.58351
		6.0	0.55816	0.02135	26.14270
		8.0	0.62165	0.01693	36.72180
		10.0	0.67646	0.01344	50.33482
		12.0	0.72182	0.01079	[illegible]
		14.0	0.75884	0.00877	[illegible]
		16.0	0.78898	0.00724	[illegible]
		18.0	0.81356	0.00604	[illegible]
		20.0	0.83373	0.00512	[illegible]

TABLE I (CONTINUED)

VARIATION OF DISPLACEMENT THICKNESS RATIO, $\frac{\delta^*}{\delta}$, MOMENTUM THICKNESS RATIO, $\frac{\theta}{\delta}$, AND BOUNDARY LAYER SHAPE PARAMETER WITH MACH NUMBER, M, AND HEAT TRANSFER PARAMETER, $\frac{T_w - T_e}{T_\infty}$, FOR A VELOCITY PROFILE EXPONENT, n, OF 5.0

n	$\frac{T_w - T_e}{T_\infty}$	M_∞	$\frac{\delta^*}{\delta}$	$\frac{\theta}{\delta}$	H
5.0	-2.0	4.0	0.39103	0.07235	5.39766
		6.0	0.57218	0.04215	13.57533
		8.0	0.68086	0.02735	24.89580
		10.0	0.75159	0.01909	39.37140
		12.0	0.80032	0.01404	57.00142
		14.0	0.83[illegible]37	0.01074	77.78399
		16.0	0.86144	0.00847	101.70017
		18.0	0.88135	0.00684	128.83985
		20.0	0.89688	0.00563	159.30728
5.0	-4.0	6.0	0.53339	0.04843	11.01383
		8.0	0.68386	0.02966	23.37894
		10.0	0.74283	0.02013	38.89031
		12.0	0.79313	0.01437	54.87790
		14.0	0.83216	0.01105	75.31222
		16.0	0.85934	0.00865	99.34104
		18.0	0.87892	0.00695	126.60432
		20.0	0.89387	0.00571	156.90018
5.0	-6.0	6.0	0.48265	0.05738	8.41234
		8.0	0.64380	0.03242	19.85811
		10.0	0.73280	0.02131	34.38761
		12.0	0.78963	0.01516	52.08443
		14.0	0.82879	0.01137	72.89358
		16.0	0.85716	0.00884	96.98833
		18.0	0.87844	0.00708	124.06780
		20.0	0.89483	0.00580	154.27586
5.0	-8.0	8.0	0.62047	0.03583	17.31789
		10.0	0.72106	0.02263	31.90455
		12.0	0.78372	0.01580	49.60127
		14.0	0.82525	0.01172	70.41809
		16.0	0.85480	0.00905	94.46409
		18.0	0.87691	0.00721	121.62275
		20.0	0.89377	0.00588	152.00680
5.0	-10.0	8.0	0.59244	0.04019	14.73999
		10.0	0.70091	0.02416	29.36328
		12.0	0.77738	0.01650	[illegible]
		14.0	0.82152	0.01209	[illegible]
		16.0	0.85253	0.00927	91.[illegible]
		18.0	0.87534	0.00735	119.08844
		20.0	0.89768	0.00597	149.53099

VARIATION OF DISPLACEMENT THICKNESS RATIO, $\frac{\delta^*}{\delta}$, MOMENTUM THICKNESS RATIO, $\frac{\theta}{\delta}$, AND BOUNDARY LAYER SHAPE PARAMETER WITH MACH NUMBER, M, AND HEAT TRANSFER PARAMETER, $\frac{T_w - T_e}{T_\infty}$, FOR A VELOCITY PROFILE EXPONENT, n, OF 7.0

n	$\frac{T_w - T_e}{T_\infty}$	M_∞	$\frac{\delta^*}{\delta}$	$\frac{\theta}{\delta}$	H
7.0	-2.0	4.0	0.32871	0.06304	5.21418
		6.0	0.50724	0.03868	13.11272
		8.0	0.62259	0.02588	24.05719
		10.0	0.70087	0.01841	38.07170
		12.0	0.75632	0.01372	55.12391
		14.0	0.79702	0.01057	75.40208
		16.0	0.82773	0.00839	98.65318
		18.0	0.85145	0.00681	125.03871
		20.0	0.87011	0.00568	153.72798
7.0	-4.0	6.0	0.46897	0.04178	10.70400
		8.0	0.60472	0.02784	21.[illegible]
		10.0	0.69094	0.01932	35.76087
		12.0	0.75044	0.01410	52.98231
		14.0	0.79330	0.01085	73.11521
		16.0	0.82526	0.00859	96.07583
		18.0	0.84974	0.00693	122.61183
		20.0	0.86890	0.00572	151.90559
7.0	-6.0	6.0	0.41892	0.05066	8.26885
		8.0	0.58326	0.03019	19.37097
		10.0	[illegible]	0.02036	33.40373
		12.0	0.74418	0.01473	50.52274
		14.0	0.78940	0.01118	70.73477
		16.0	0.82270	0.00875	94.02288
		18.0	0.84789	0.00705	120.28369
		20.0	0.86706	0.00579	149.86183
7.0	-8.0	8.0	0.55900	0.03303	16.92401
		10.0	0.66824	0.02153	31.03570
		12.0	[illegible]	0.01531	48.17113
		14.0	0.78532	0.01148	68.40597
		16.0	0.82005	0.00894	91.73378
		18.0	0.84619	0.00717	118.01953
		20.0	0.86619	0.00587	147.50796
7.0	-10.0	8.0	0.53041	0.03656	14.50766
		10.0	0.65536	0.02285	28.67396
		12.0	0.73040	0.01593	45.85080
		14.0	0.78104	0.01182	66.07448
		16.0	0.81729	0.00915	89.32240
		18.0	0.84433	0.00729	115.81619
		20.0	0.86509	0.00596	145.15101

TABLE I (CONCLUDED)

VARIATION OF DISPLACEMENT THICKNESS RATIO, $\frac{\delta^*}{\delta}$, MOMENTUM THICKNESS RATIO, $\frac{\theta}{\delta}$, AND BOUNDARY LAYER SHAPE PARAMETER WITH MACH NUMBER, M, AND HEAT TRANSFER PARAMETER, $\frac{T_w - T_e}{T_\infty}$, FOR A VELOCITY PROFILE EXPONENT, n, OF 9.0

n	$\frac{T_w - T_e}{T_\infty}$	M_∞	$\frac{\delta^*}{\delta}$	$\frac{\theta}{\delta}$	H
9.0	-2.0	4.0	0.28455	0.05567	5.11227
		6.0	0.45794	0.03561	12.85875
		8.0	0.57028	0.02440	23.61885
		10.0	0.65932	0.01762	37.41771
		12.0	0.71850	0.01327	54.22005
		14.0	0.76438	0.01031	74.14161
		16.0	0.79868	0.00824	96.92961
		18.0	0.82538	0.00672	122.82738
		20.0	0.84856	0.00558	151.72043
9.0	-4.0	6.0	0.41954	0.03982	10.33491
		8.0	0.55729	0.02614	21.31982
		10.0	0.64874	0.01847	35.12182
		12.0	0.71311	0.01372	51.97522
		14.0	0.76028	0.01058	71.88200
		16.0	0.79391	0.00840	94.75000
		18.0	0.82346	0.00684	120.39474
		20.0	0.84519	0.00565	149.39292
9.0	-6.0	6.0	0.37196	0.04542	8.19022
		8.0	0.53582	0.02818	19.02899
		10.0	0.63726	0.01940	32.85052
		12.0	0.70633	0.01421	49.70443
		14.0	0.75509	0.01087	69.54922
		16.0	0.79305	0.00859	92.32829
		18.0	0.82149	0.00695	118.20144
		20.0	0.84[illegible]9	0.00572	147.51748
9.0	-8.0	8.0	0.51122	0.03089	16.71134
		10.0	0.62475	0.02044	30.56751
		12.0	0.69912	0.01475	47.39661
		14.0	0.78150	0.01117	67.27842
		16.0	0.79010	0.00877	90.09122
		18.0	0.81947	0.00705	116.24113
		20.0	0.84235	0.00580	145.24138
9.0	-10.0	8.0	0.48883	0.03384	14.38870
		10.0	0.61104	0.02161	28.27395
		12.0	0.69145	0.01532	45.13708
		14.0	0.74880	0.01149	64.99565
		16.0	0.78704	0.00896	87.83482
		18.0	0.81738	0.00718	113.84401
		20.0	0.84087	0.00590	142.52542

VARIATION OF DISPLACEMENT THICKNESS RATIO, $\frac{\delta^*}{\delta}$, MOMENTUM THICKNESS RATIO, $\frac{\theta}{\delta}$, AND BOUNDARY LAYER SHAPE PARAMETER WITH MACH NUMBER, M, AND HEAT TRANSFER PARAMETER, $\frac{T_w - T_e}{T_\infty}$, FOR A VELOCITY PROFILE EXPONENT, n, OF 11.0

n	$\frac{T_w - T_e}{T_\infty}$	M_∞	$\frac{\delta^*}{\delta}$	$\frac{\theta}{\delta}$	H
11.0	-2.0	4.0	0.25150	0.04986	5.04412
		6.0	0.41870	0.03296	12.89172
		8.0	0.53803	0.02306	23.33044
		10.0	0.62414	0.01689	36.95086
		12.0	0.68774	0.01284	53.55919
		14.0	0.73583	0.01006	73.14115
		16.0	0.77296	0.00806	95.90571
		18.0	0.80212	0.00660	121.53030
		20.0	0.82537	0.00550	150.07273
11.0	-4.0	6.0	0.38118	0.03658	10.42100
		8.0	0.51874	0.02459	21.09394
		10.0	0.61312	0.01765	34.73654
		12.0	0.68097	0.01325	51.39623
		14.0	0.73143	0.01031	70.94083
		16.0	0.76998	0.00823	93.88019
		18.0	0.80003	0.00671	119.22504
		20.0	0.82387	0.00557	147.91741
11.0	-6.0	6.0	0.33548	0.04123	8.13728
		8.0	0.49707	0.02639	18.83668
		10.0	0.60121	0.01850	32.49730
		12.0	0.67381	0.01370	49.18248
		14.0	0.72685	0.01057	68.77010
		16.0	0.76692	[illegible]	91.51551
		18.0	0.79789	[illegible]	116.99413
		20.0	0.82233	0.00564	145.79787
11.0	-8.0	8.0	0.47246	0.02850	16.57898
		10.0	0.58828	0.01944	30.26235
		12.0	0.66820	0.01421	46.88248
		14.0	0.72205	0.01085	66.55300
		16.0	0.76371	0.00858	89.21729
		18.0	0.79567	0.00693	114.81962
		20.0	0.82075	0.00572	143.49650
11.0	-10.0	8.0	0.44414	0.03104	14.30735
		10.0	0.57417	0.02049	28.02343
		12.0	0.65815	0.01473	44.87783
		14.0	0.71702	0.01115	64.30493
		16.0	0.76040	0.00874	87.00239
		18.0	0.79341	0.00704	112.69886
		20.0	0.81914	0.00581	140.98107

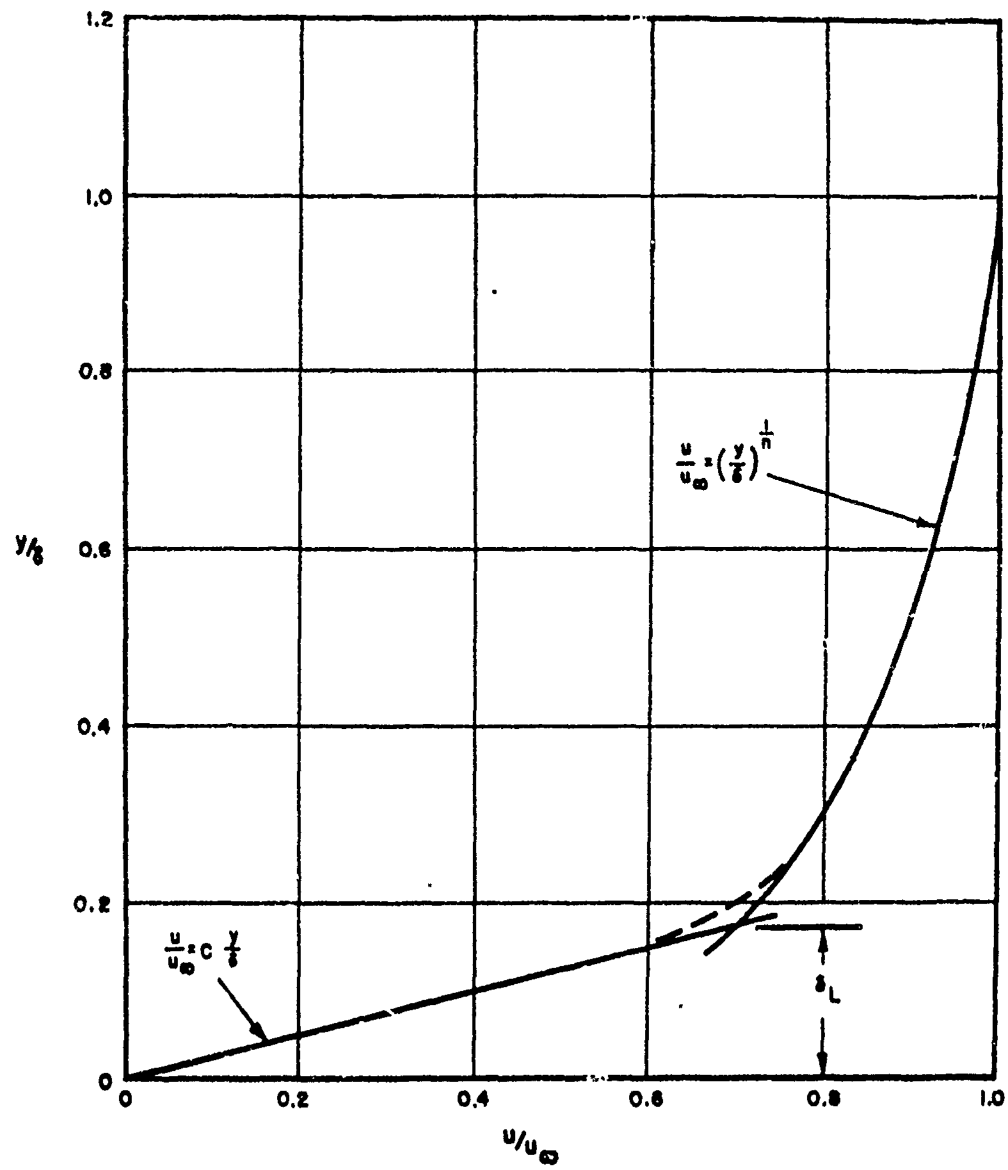

FIG. I VELOCITY DISTRIBUTION ACROSS A TYPICAL TURBULENT BOUNDARY LAYER

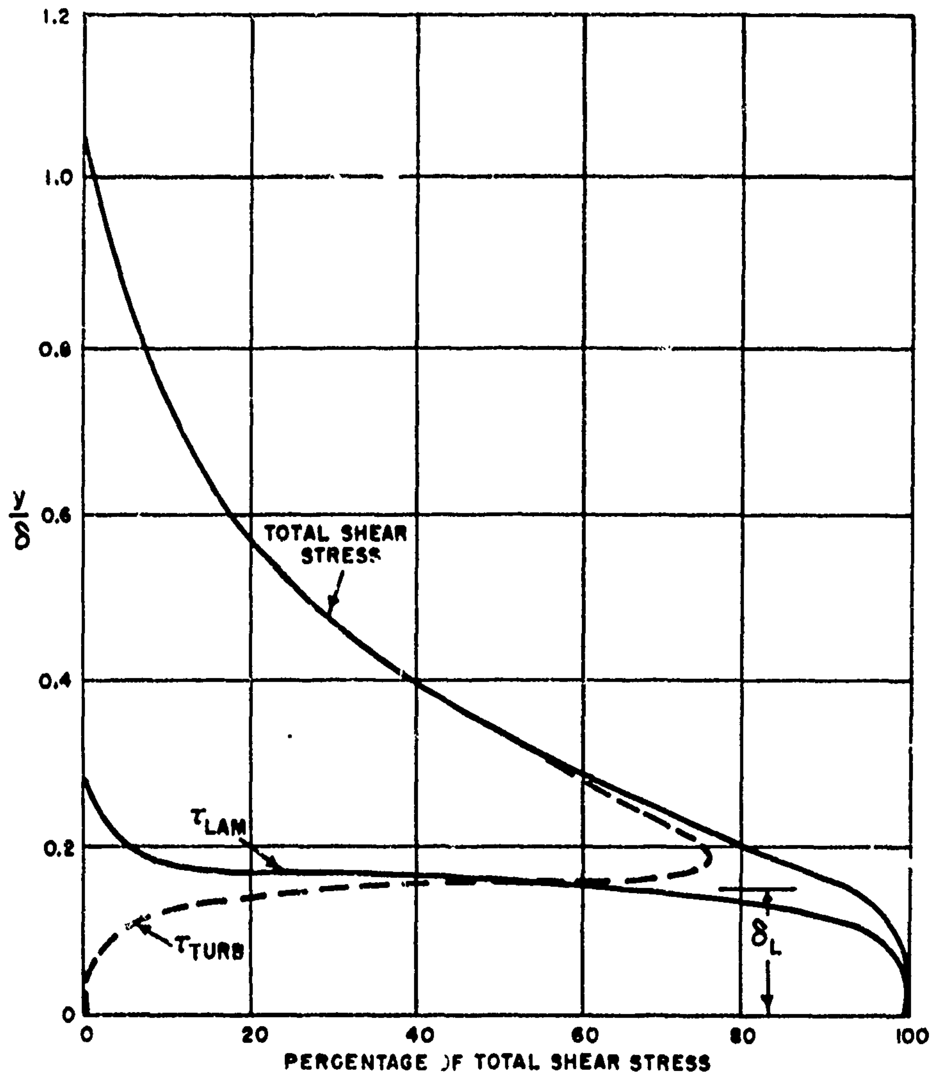

FIG. 2 SCHEMATIC VIEW OF VISCOUS AND TURBULENT SHEAR STRESS ACROSS A TYPICAL TURBULENT BOUNDARY LAYER

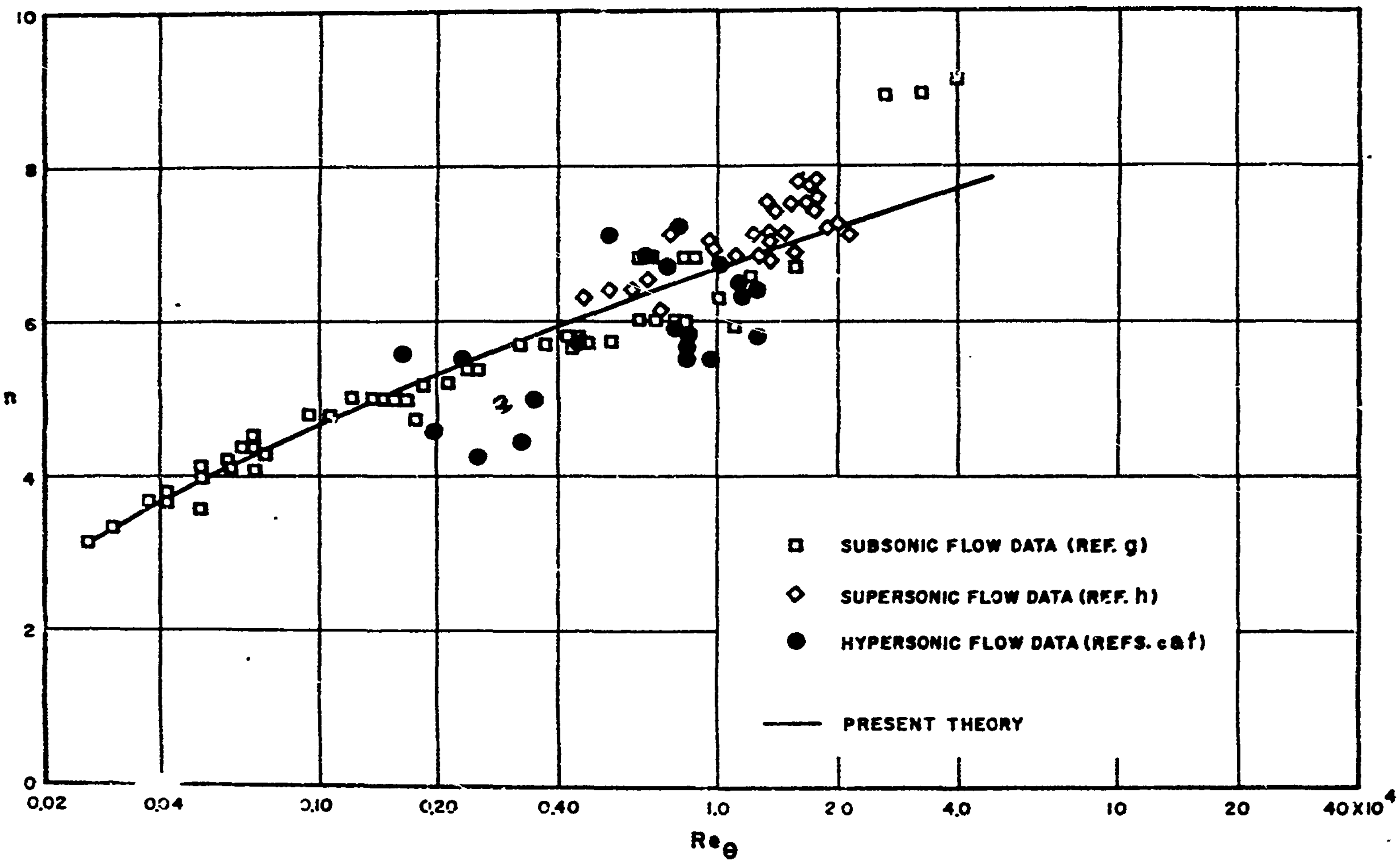

F 3.3 VARIATION OF TURBULENT BOUNDARY LAYER VELOCITY PROFILE EXPONENT (n) WITH REYNOLDS NUMBER (Re_θ)

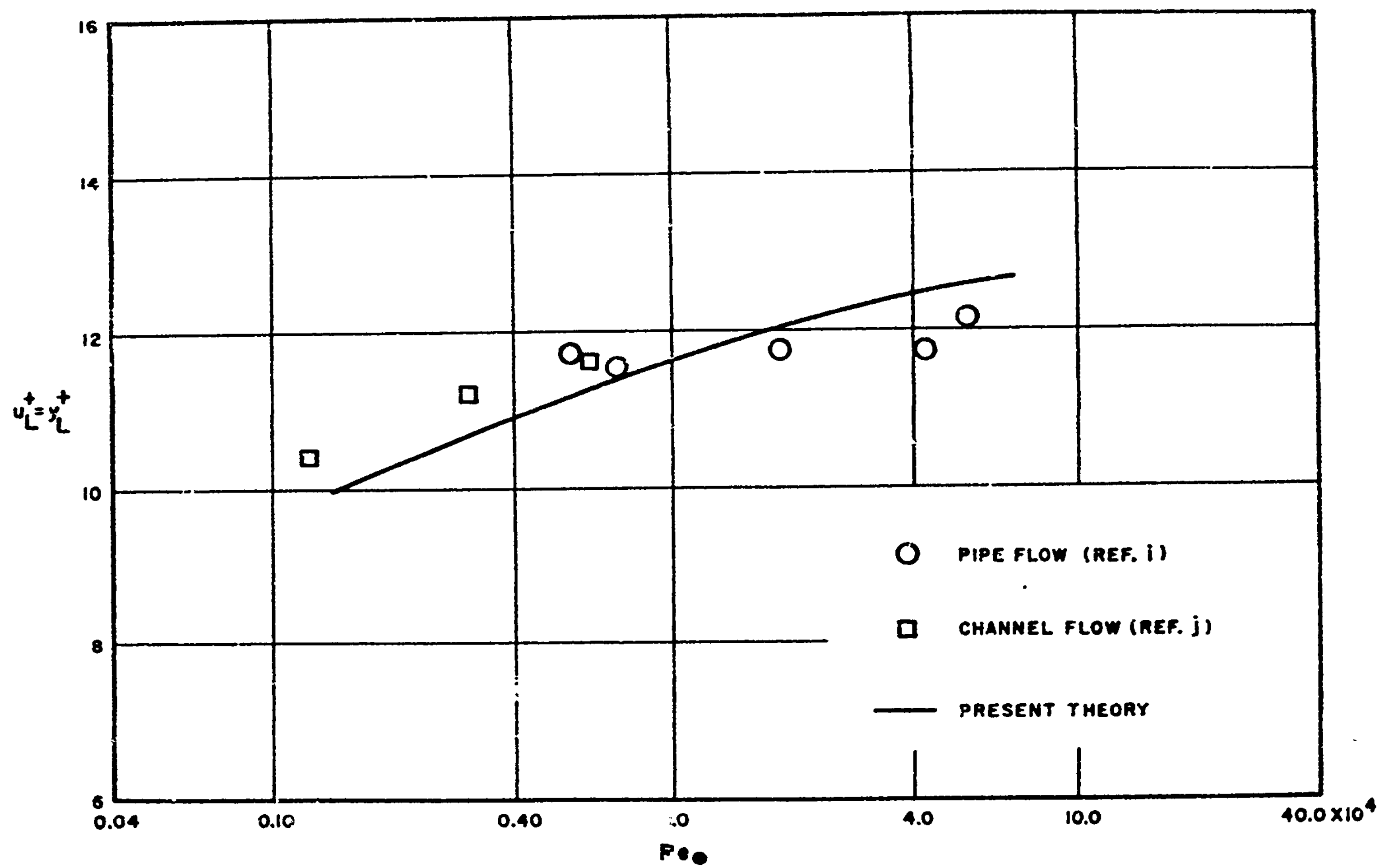

FIG. 4 VARIATION OF $u_L^+ = y_L^+$ WITH REYNOLDS NUMBER (Re_θ) FOR INCOMPRESSIBLE FLOW

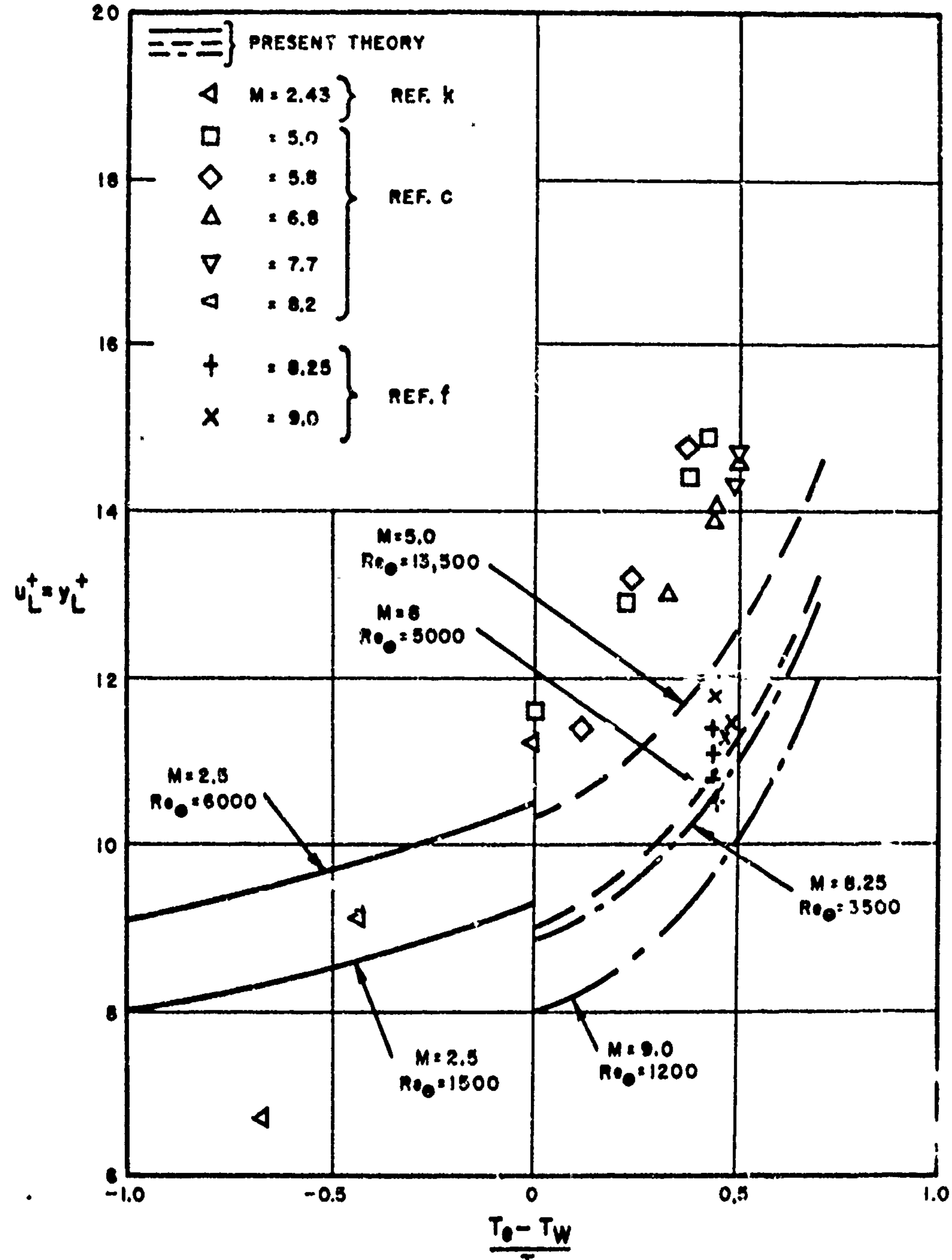

FIG. 5 COMPARISON BETWEEN THEORETICAL AND EXPERIMENTAL VALUES OF $u_L^+ = y_L^+$ FOR COMPRESSIBLE FLOW

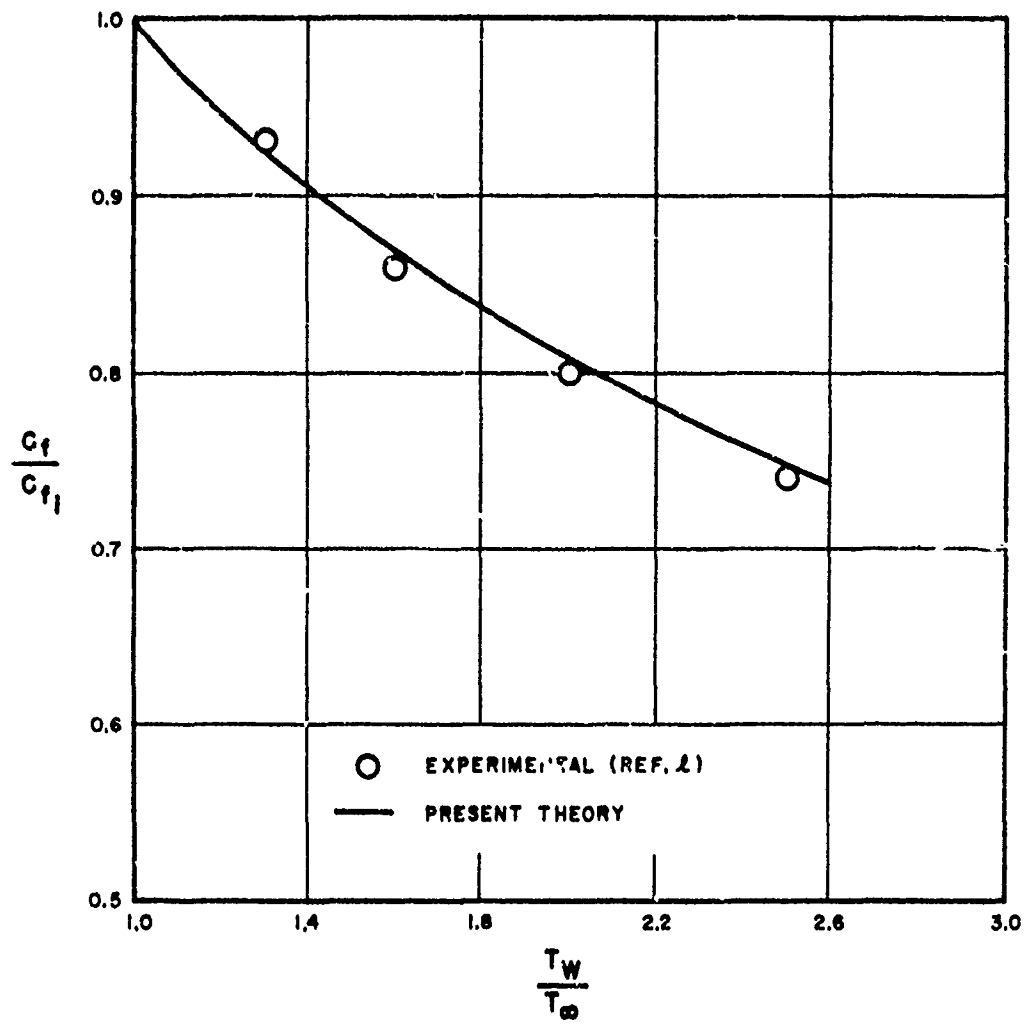

FIG. 6 INFLUENCE OF HEAT TRANSFER ON SKIN FRICTION RATIO FOR INCOMPRESSIBLE FLOW

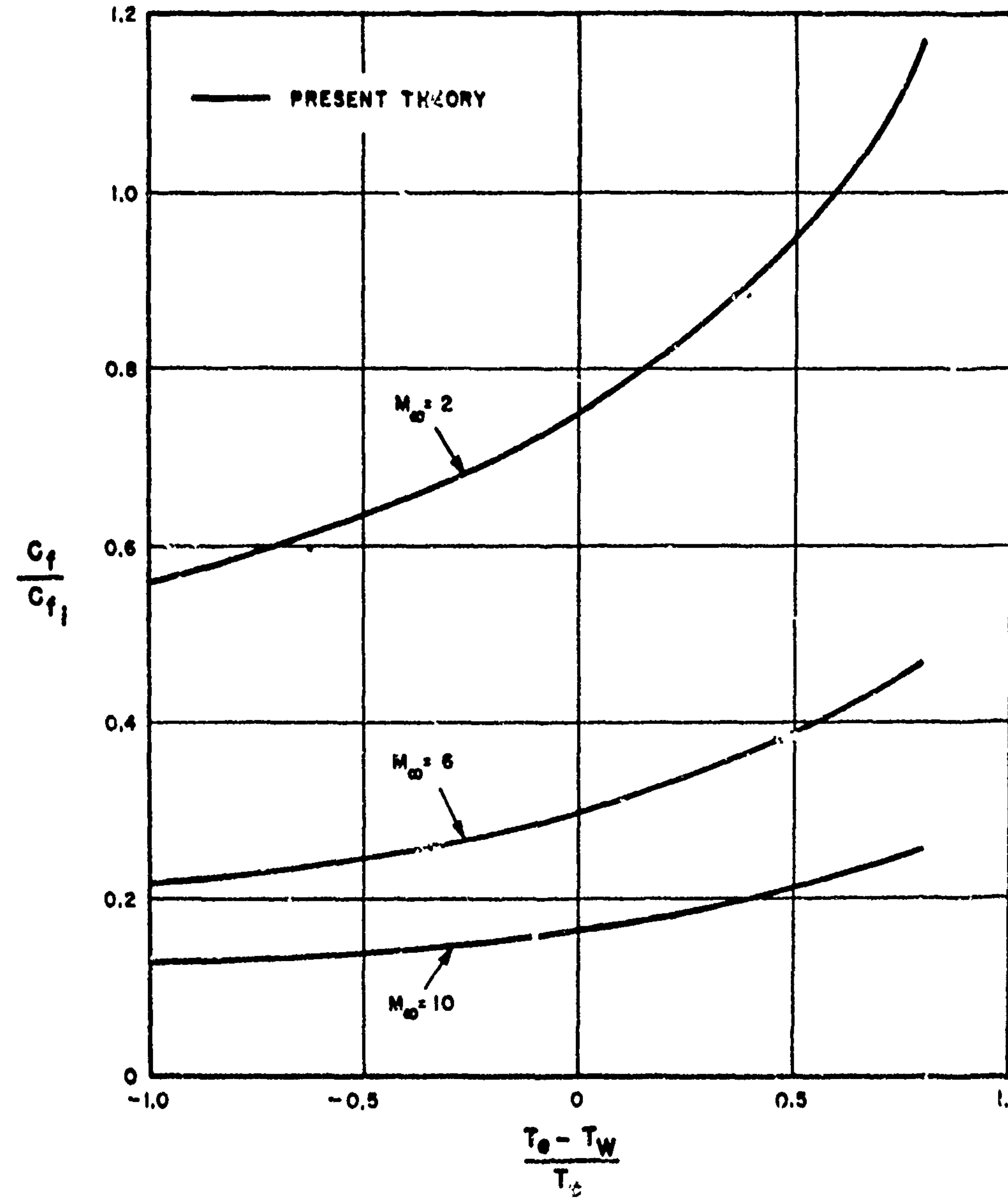

FIG. 7 INFLUENCE OF HEAT TRANSFER ON SKIN FRICTION RATIO FOR THREE VALUES OF MACH NUMBER AND $Re_e = 13{,}500$

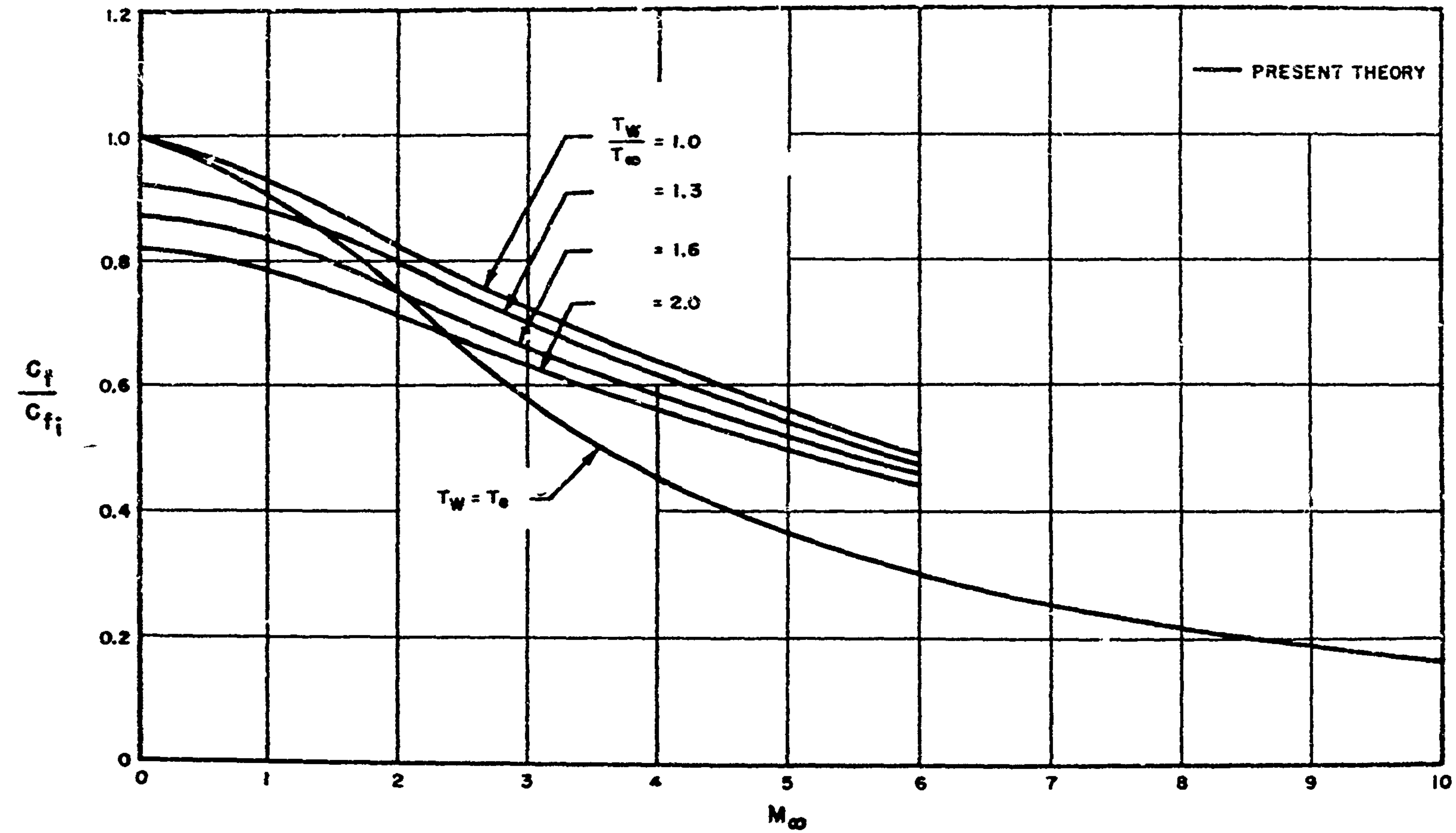

FIG. 8 VARIATION OF SKIN FRICTION RATIO WITH MACH NUMBER FOR SEVERAL CONSTANT VALUES OF WALL TO FREE STREAM TEMPERATURE RATIO AND Re_Θ=13,500

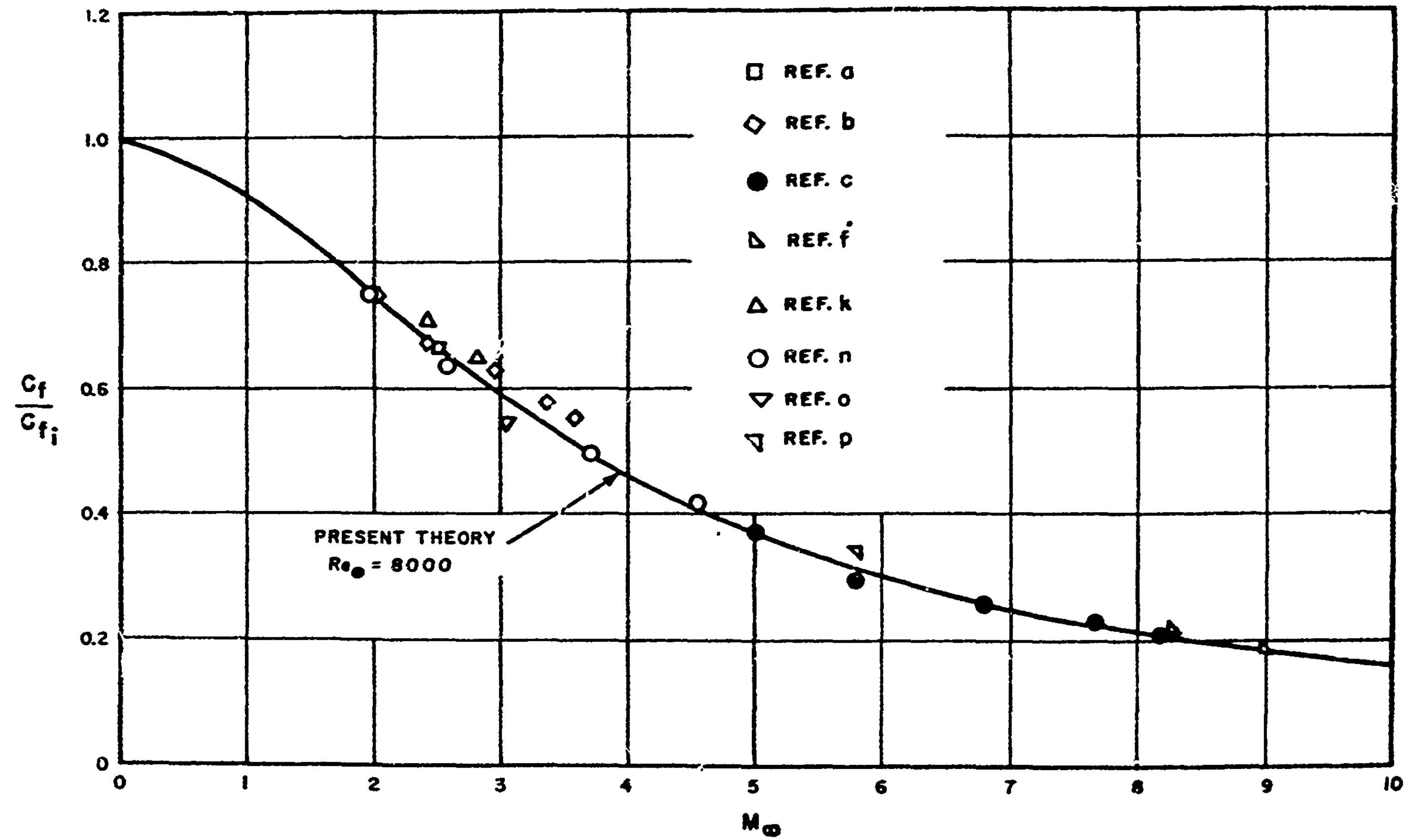

FIG. 9 VARIATION OF SKIN FRICTION RATIO WITH MACH NUMBER FOR ZEFO HEAT TRANSFER AND Re_θ =8000

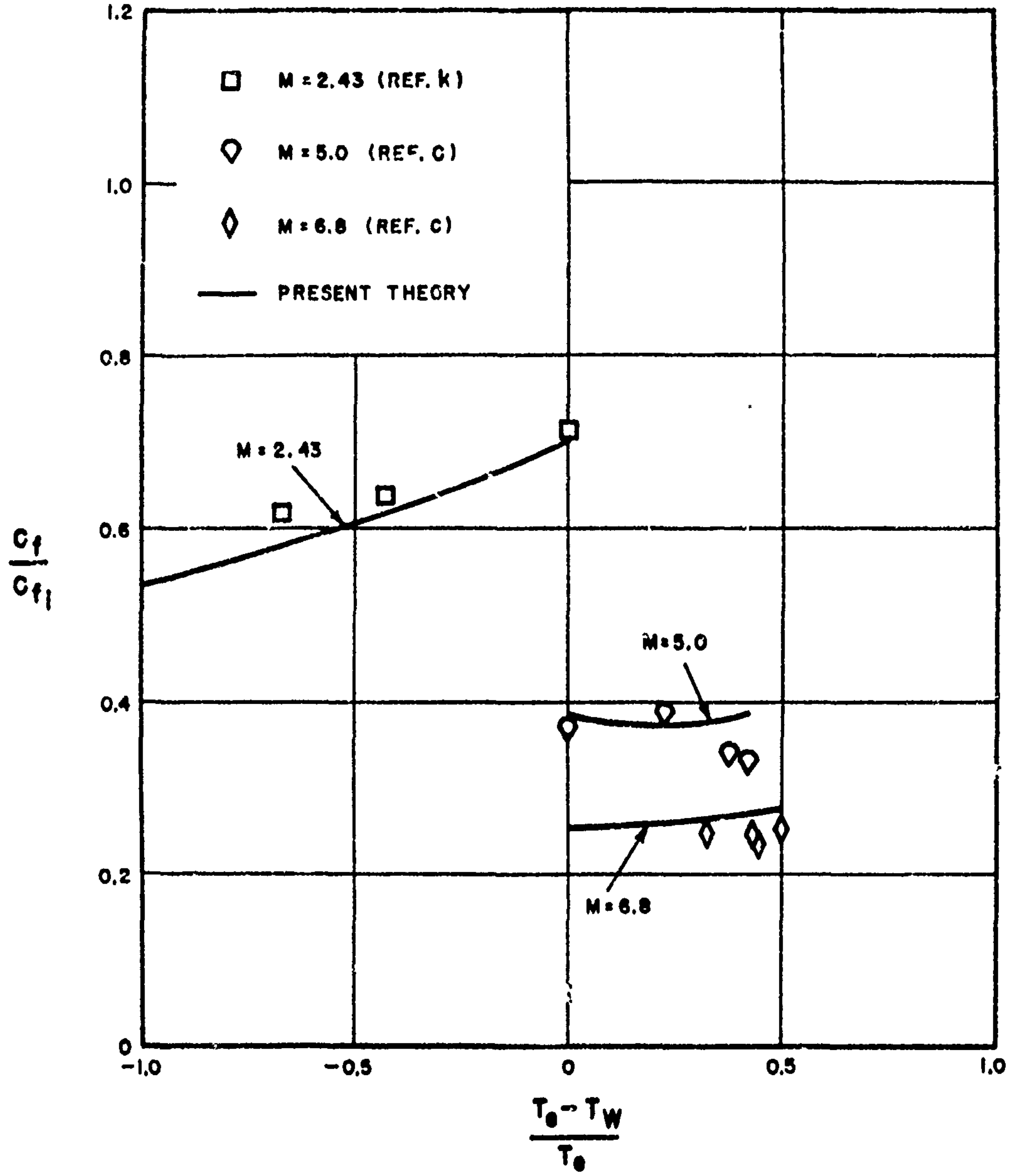

FIG. 10 COMPARISON BETWEEN THEORETICAL AND EXPERIMENTAL VALUES OF SKIN FRICTION RATIO FOR M=2.43, 5.0 AND 6.8

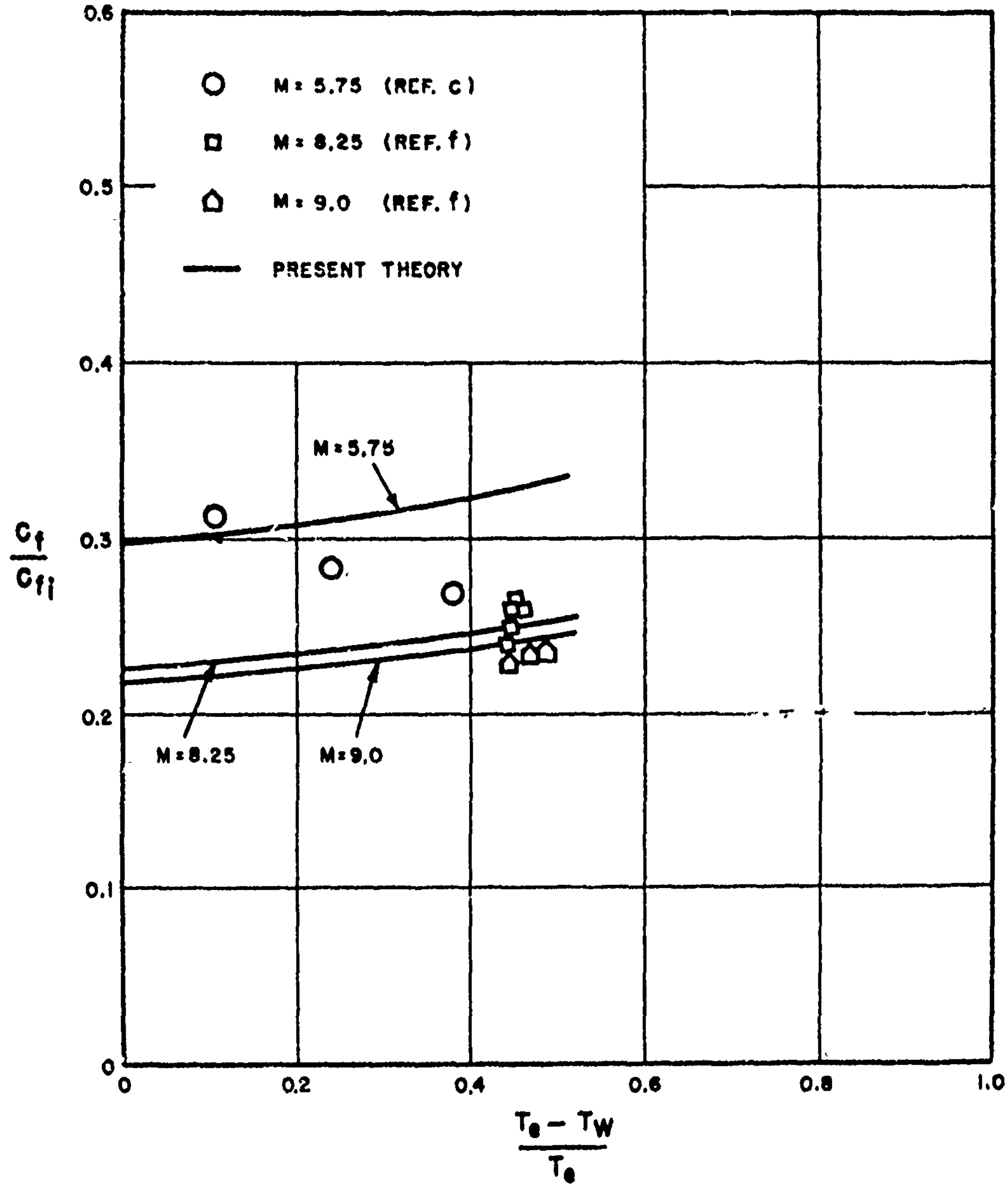

FIG. 11 COMPARISON BETWEEN THEORETICAL AND EXPERIMENTAL VALUES OF SKIN FRICTION RATIO FOR M = 5.75, 8.25, AND 9.0

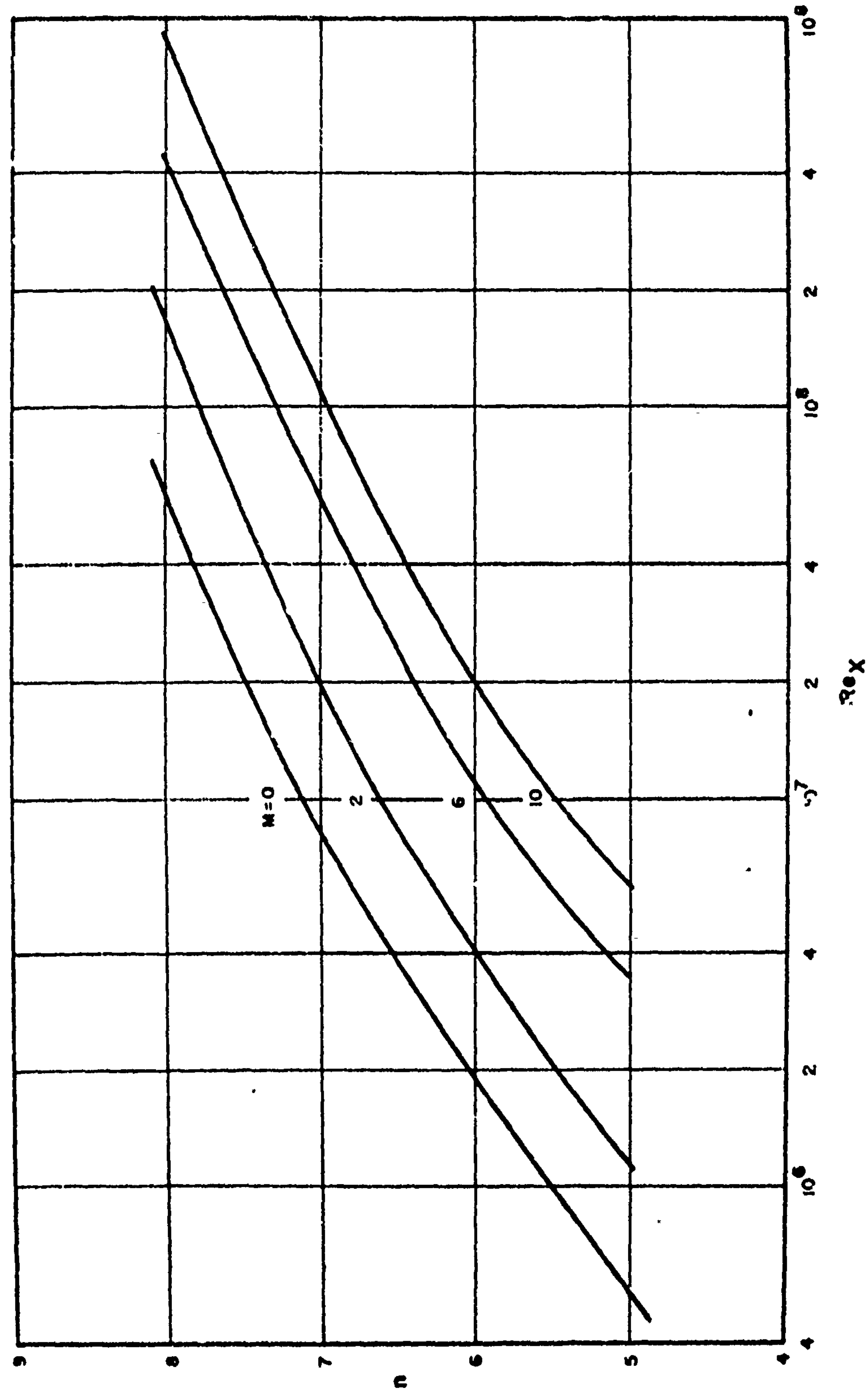

FIG.12 VARIATION OF n WITH Re_X FOR SEVERAL CONSTANT VALUES OF MACH NUMBER

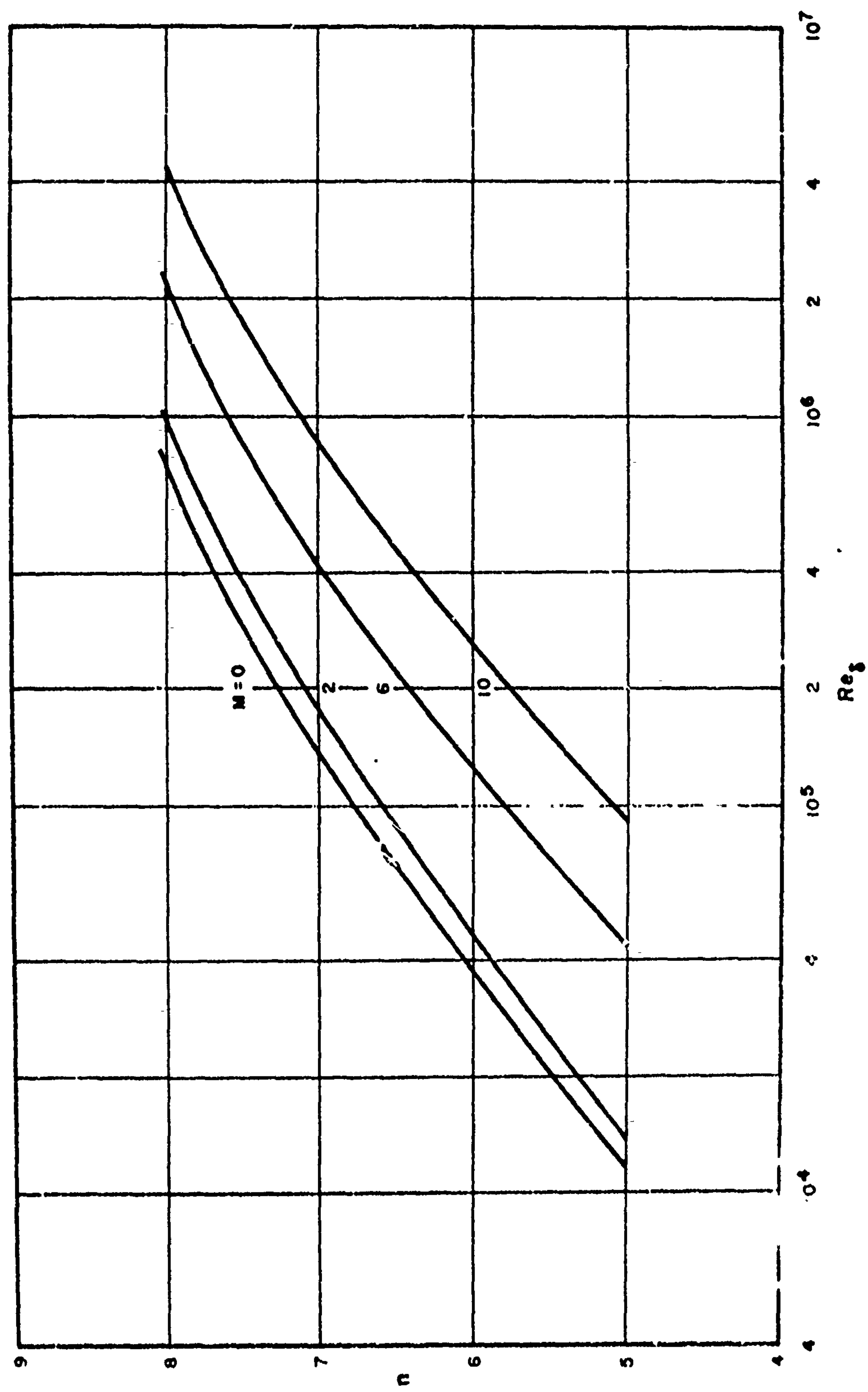

FIG. 13 VARIATION OF n WITH Re_δ FOR SEVERAL CONSTANT VALUES OF MACH NUMBER

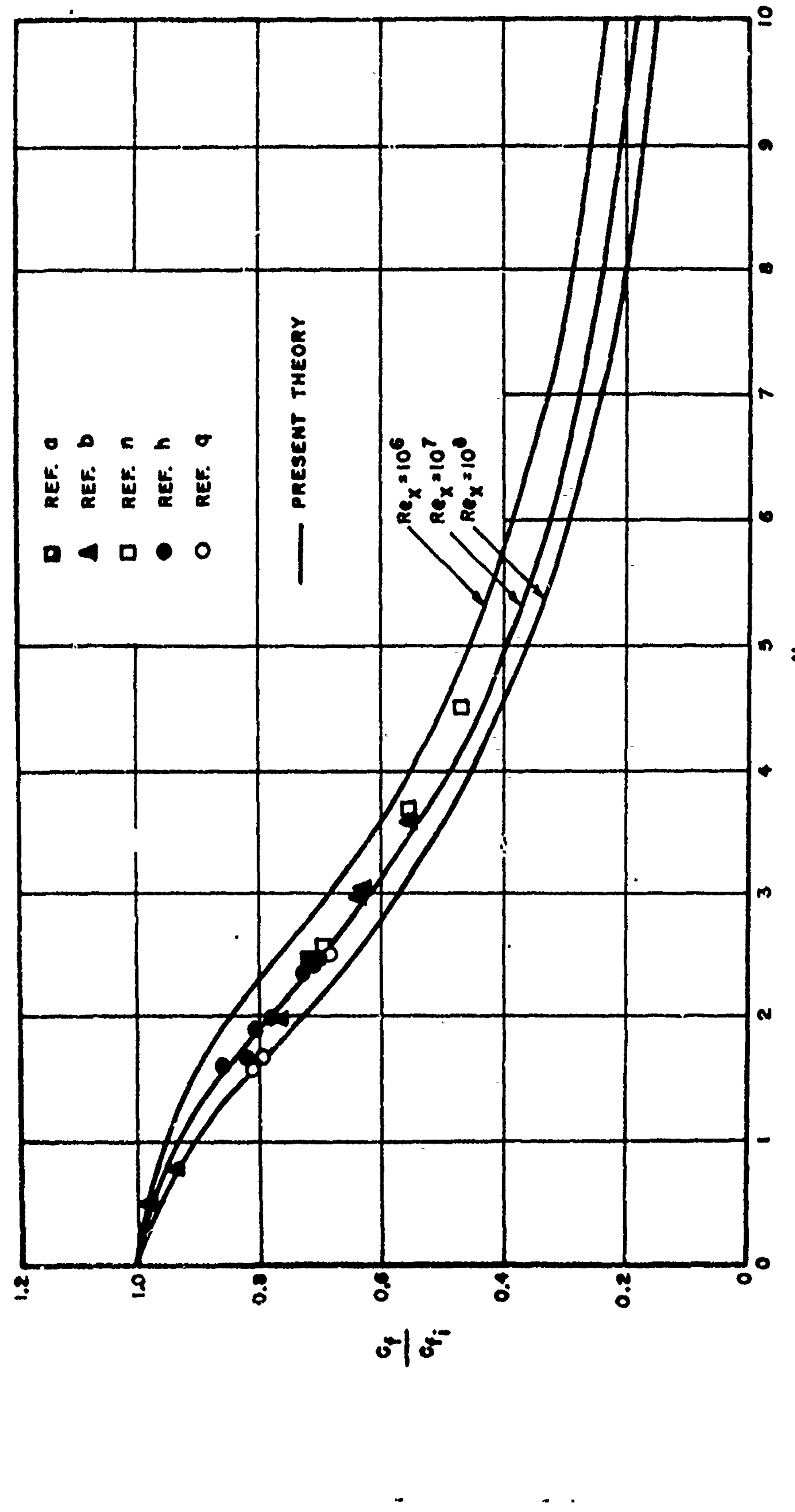

FIG. 14 VARIATION OF SKIN FRICTION RATIO WITH MACH NUMBER FOR CONSTANT VALUES OF Re_x OF 10^6, 10^7, AND 10^8

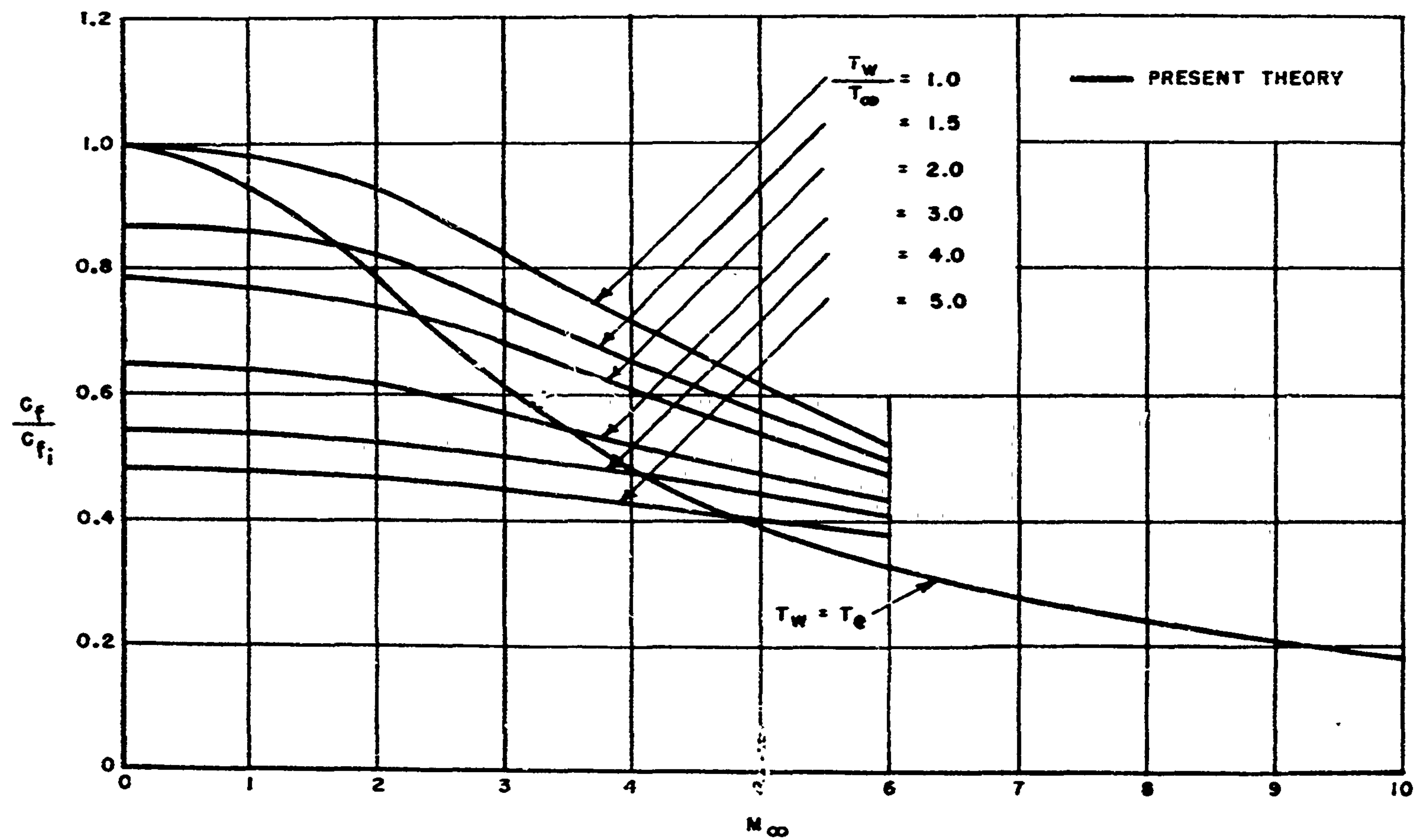

FIG. 15 VARIATION OF SKIN FRICTION RATIO WITH MACH NUMBER FOR SEVERAL CONSTANT VALUES OF WALL TO FREE-STREAM TEMPERATURE RATIO AND A CONSTANT Re_x OF 10^7

Aeroballistic Research Department
External Distribution List for Aeroballistics Research (XI)

No. of Copies	
	Chief, Bureau of Ordnance Department of the Navy Washington 25, D. C.
1	Attn: Re3d
2	Attn: Re6
2	Attn: Re9a
	Chief, Bureau of Aeronautics Department of the Navy Washington 25, D. C.
1	Attn: AER-TD-414
2	Attn: RS-7
	Commander U. S. Naval Ordnance Test Station Inyokern P. O. China Lake, California
2	Attn: Technical Library
1	Attn: Code 5003
	Commander U. S. Naval Air Missile Test Center Point Mugu, California
2	Attn: Technical Library
	Superintendent U. S. Naval Postgraduate School Monterey, California
1	Attn: Librarian
	Commanding Officer and Director David Taylor Model Basin Washington 7, D. C.
2	Attn: Hydrodynamics Laboratory
	Chief of Naval Research Library of Congress Washington 25, D. C.
2	Attn: Technical Info. Div.
	Office of Naval Research Department of the Navy Washington 25, D. C.
1	Attn: Code 438
2	Attn: Code 463

No. of Copies	
	National Bureau of Standards
	Washington 25, D. C.
1	Attn: Nat'l Applied Math. Lab.
1	Attn: Librarian (Ord. Dev. Div.)
1	Attn: Chief, Mechanics Div.
	National Bureau of Standards
	Corona Laboratories (Ord. Dev. Div.)
	Corona, California
1	Attn: Dr. H. Thomas
	University of California
	211 Mechanics Building
	Berkeley 4, California
1	Attn: Mr. G. J. Maslach
1	Attn: Dr. S. A. Schaaf
2	Commanding General
	Redstone Arsenal
	Huntsville, Alabama
	Attn: Tech. Library
1	Jet Propulsion Lab.
	California Institute of Technology
	4800 Oak Grove Drive
	Pasadena 3, California
	Attn: F. E. Goddard, Jr.
	California Institute of Technology
	Pasadena 4, California
2	Attn: Librarian (Guggenheim Aero Lab)
1	Attn: Dr. H. T. Nagamatsu
1	Attn: Prof. M. S. Plesset
1	Attn: Dr. Hans W. Liepmann
	VIA: BuAer Representative
	University of Illinois
	202 E. E. R. L.
	Urbana, Illinois
1	Attn: Prof. A. H. Taub
1	Director
	Inst. for Fluid Dynamics and Applied Math
	University of Maryland
	College Park, Maryland
	Massachusetts Inst. of Technology
	Cambridge 39, Massachusetts
1	Attn: Prof. G. Stever
1	Attn: Prof. J. Kaye

No. of Copies	
	University of Michigan Ann Arbor, Michigan
1	Attn: Prof. Otto Laporte
	University of Michigan Willow Run Research Center Ypsilanti, Michigan
1	Attn: L. R. Biasell
	Dept. of Mechanical Engr. University of Minnesota Institute of Technology Minneapolis 14, Minnesota
1	Attn: Prof. N. A. Hall
	The Ohio State University Columbus, Ohio
2	Attn: G. L. Von Eschen
	Polytechnic Institute of Brooklyn Aerodynamics Laboratory 527 Atlantic Avenue Freeport, New York
1	Attn: Dr. Antonio Ferri VIA: ONR
	Massachusetts Inst. of Technology Cambridge 39, Massachusetts
2	Attn: Project Meteor
1	Attn: Guided Missiles Library
1	Princeton University Forrestal Research Center Library Project Squid Princeton, New Jersey
	Armour Research Foundation 35 West 33rd Street Chicago 16, Illinois
1	Attn: Engr. Mech. Div. VIA: ONR
	Princeton University Princeton, New Jersey
1	Attn: Prof. S. Bogdonoff VIA: ONR

No. of Copies	
	Applied Physics Laboratory The Johns Hopkins University 8621 Georgia Avenue Silver Spring, Maryland
1	Attn: Arthur G. Norris VIA: NIO
1	Cornell Acronautical Lab., Inc. 4455 Genesee Street Buffalo 21, New York VIA: BuAer Rep.
1	Defense Research Laboratory University of Texas Box 1, University Station Austin, Texas
	Eastman Kodak Company 50 W. Main Street Rochester 4, New York
1	Attn: Dr. Herbert Trotter, Jr. VIA: NIO
	General Electric Company Building #1, Campbell Ave. Plant Schenectady, New York
1	Attn: Joseph C. Hoffman VIA: InsMachinery
	The Rand Corporation 1700 Main Street Santa Monica, California
1	Attn: The Librarian
	Consolidated Vultee Aircraft Corp. Daingerfield, Texas
1	Attn: J. E. Arnold VIA: Dev. Contract Office
	Douglas Aircraft Company, Inc. 3000 Ocean Park Boulevard Santa Monica, California
1	Attn: Mr. E. F. Burton VIA: BuAer Resident Rep.
1	BuAer Representative AeroJet--General Corp. 6352 North Irwindale Ave. Azusa, California

No. of Copies	
	North American Aviation, Inc. 12214 Lakewood Boulevard Downey, California
2	Attn: Aerophysics Library
	VIA: BuAer Representative
	United Aircraft Corporation East Hartford 8, Connecticut
1	Attn: Robert C. Sale
	VIA: BuAer Representative
	National Advisory Committee for Aero. 1512 H Street, Northwest Washington 25, D. C.
5	Attn: E. B. Jackson
	Ames Aeronautical Laboratory Moffett Field, California
1	Attn: H. J. Allen
2	Attn: Dr. A. C. Charters
	NACA Lewis Flight Propulsion Lab Cleveland Hopkins Airport Cleveland 11, Ohio
1	Attn: John C. Evvard
	Langley Aeronautical Laboratory Langley Field, Virginia
1	Attn: Theoretical Aerodynamics Div.
1	Attn: J. V. Becker
1	Attn: Dr. Adolf Buseman
1	Attn: Mr. C. H. McLellan
1	Attn: Mr. J. Stack
	Harvard University 21 Vanserg Building Cambridge 38, Massachusetts
1	Attn: Prof. Garrett Birkhoff
	The Johns Hopkins University Charles and 34th Streets Baltimore 18, Maryland
1	Attn: Dr. Francis H. Clauser
	New York University 45 Fourth Avenue New York 3, New York
1	Attn: Professor R. Courant

No. of Copies	
1	Dr. Allen E. Puckett, Head Missile Aerodynamics Department Hughes Aircraft Company Culver City, California
1	Dr. Gordon N. Patterson, Director Institute of Aerophysics University of Toronto Toronto 5, Ontario, Canada VIA: BuOrd (Ad8)
1	Acroon, Inc. 385 E. Green Street Pasadena 1, California VIA: Inspector of Naval Mat'l 1206 S. Santee Street Los Angeles 15, Calif.
1	Engineering Research Inst. East Engineering Building Ann Arbor, Michigan Attn: Director of Icing Research

Aeroballistic Research Department
External Distribution List for Aeroballistics Research (XIa)

No. of Copies	
6	Office of Naval Research Branch Office Navy 100 Fleet Post Office New York, New York
	Commanding General Aberdeen Proving Ground Aberdeen, Maryland
1	Attn: Dr. B. L. Hicks
	National Bureau of Standards Aerodynamics Section Washington 25, D. C.
1	Attn: Dr. G. B. Schubauer, Chief
	Ames Aeronautical Laboratory Moffett Field, California
1	Attn: Walter G. Vincenti
	University of California Observatory 21 Berkeley 4, California
1	Attn: Leland E. Cunningham
	Graduate School Aeronautical Engr. Cornell University Ithaca, New York
1	Attn: W. R. Sears, Director VIA: ONR
	Applied Math. and Statistics Lab. Stanford University Stanford, California
1	Attn: R. J. Langle, Associate Dir.
	University of Minnesota Dept. of Aeronautical Engr. Minneapolis, Minnesota
1	Attn: Professor R. Hermann
	Massachusetts Inst. of Technology Dept. of Mathematics, Room 2-270 77 Massachusetts Avenue Cambridge, Massachusetts
1	Attn: Prof. Eric Reissner

No. of Copies	
	Case Institute of Technology Dept. of Mechanical Engineering Cleveland, Ohio
1	Attn: Professor G. Kuerti VIA: ONR
	Harvard University 109 Pierce Hall Cambridge 38, Massachusetts
1	Attn: Professor R. von Mises

EXTERNAL DISTRIBUTION

No. of Copies	
1	Mr. A. I. Moskovitz Bureau of Ordnance (Re9a) Navy Department Washington, D. C.
1	Chief, Naval Operations Department of the Navy Washington 25, D. C.
1	The Artillery School Anti-aircraft & Guided Missiles Br. Fort Bliss, Texas Attn: Research & Analysis Sec.
1	Mr. Felix W. Fenter Defense Research Laboratory University of Texas Austin, Texas
1	Prof. R. F. Probstein Division of Engineering Brown University Providence, Rhode Island
1	Commander U. S. Naval Proving Ground Dahlgren, Virginia
1	Jet Propulsion Laboratory 4800 Oak Grove Drive Pasadena, California Attn: Dr. P. P. Wegener
1	Flight and Aerodynamics Laboratory Research Division Ordnance Missile Laboratory Redstone Arsenal Huntsville, Alabama Attn: J. L. Potter, Chief
5	U. S. Air Force Headquarters Arnold Engineering Development Center (ARDC) Tullahoma, Tennessee Attn: AEKS
1	Dr. R. H. Mills Wright Air Development Center Wright-Patterson Air Force Base Dayton, Ohio

No. of Copies	
1	Mr. Ronald Smelt Chief, Gas Dynamics Facility Arnold Research Organization, Inc. Tullahoma, Tennessee
1	Dr. Henry Nagamatsu California Institute of Technology Pasadena, California
1	Professor N. J. Hoff Polytechnic Institute of Brooklyn Brooklyn, New York
1	Dr. F. L. Wattendorf Facilities Division DCS/Development Hdqts. USAF, Room 5C368 Pentagon, Washington 25, D. C.
1	Professor A. Kantrowitz Cornell University Department of Aeronautical Engineering Ithaca, New York
1	Professor Lester Lees California Institute of Technology Pasadena, California
1	Dr. H. G. Stever MIT, Department of Aeronautical Engineering Cambridge, Massachusetts
1	Professor G. L. Von Eschen Aeronautical Engineering Department Ohio State University Columbus, Ohio
1	Mr. R. L. Bayless Consolidated Vultee Aircraft Corporation San Diego, California
1	Professor S. M. Bogdonoff Department of Aeronautical Engineering Princeton University Princeton, New Jersey
1	Professor J. Kaye MIT, Physics Department Cambridge, Massachusetts

No. of Copies	
1	Dr. Ernst R. G. Eckert Department of Mechanical Engineering University of Minnesota Minneapolis 14, Minnesota
1	Mr. Mervin Sibulkin Jet Propulsion Laboratory 4800 Oak Grove Drive Pasadena, California
1	Dr. G. R. Eber Holloman Air Force Base Alamagordo, New Mexico
1	Dr. Albert E. Lombard Pentagon, Rm. 4E348 Washington, D. C.
1	Dr. E. R. Van Driest Aerophysics Laboratory North American Aviation, Inc. Downing, California
1	Dr. Paul A. Libby Polytechnic Institute of Brooklyn 99 Livingston Street Brooklyn, New York
1	Dr. W. S. Bradfield Aero. Engr. Dept. University of Minnesota Minneapolis, Minnesota
1	Dr. D. Coles California Institute of Technology Pasadena 4, California
1	Prof. Dr. H. Reichardt Max Planck Institut fuer Stroemungsforschung Goettingen, Germany
1	Prof. Dr. H. Schlichting Institut fuer Stroemungsmechanik der Technischen Hochschule Wodanstrasse 42 Braunschweig, Germany
1	Prof. Dr. J. Ackeret Soenneggstrasse 3 Zurich 6, Switzerland

No. of Copies	
	Director
	Naval Research Laboratory
	Washington 25, D. C.
1	Attn: Code 2021
1	Attn: Code 3800
	Office, Chief of Ordnance
	U. S. Army
	Washington 25, D. C.
1	Attn: ORDTU
2	Library Branch
	Research and Development Board
	Pentagon 3D1041
	Washington 25, D. C.
	Chief, AFSWP
	P. O. Box 2610
	Washington 25, D. C.
1	Attn: Technical Library
1	Chief, Physical Vulnerability Branch
	Air Targets Division
	Directorate of Intelligence
	Headquarters, USAF
	Washington 25, D. C.
	Commanding General
	Wright Air Development Center
	Wright-Patterson Air Force Base
	Dayton, Ohio
5	Attn: WCACD
1	Attn: WCSD
2	Attn: WCSOR
2	Attn: WCRRN
1	Attn: WCACD
1	Attn: WCRRF
2	Attn: WCLGH
1	Director
	Air University Library
	Maxwell Air Force Base, Alabama
	Commanding General
	Aberdeen Proving Ground
	Aberdeen, Maryland
1	Attn: C. L. Poor
1	Attn: D. S. Dederick

No. of Copies	
1	D. N. Morris Douglas Aircraft Company, Inc. El Segundo Division El Segundo, California
1	K. E. Van Every Douglas Aircraft Company, Inc. El Segundo Division El Segundo, California
1	Dr. G. V. Bull Canadian Armament Research and Development Establishment P. O. Box 1427 Quebec, Quebec, Canada
2	Dr. Philip A. Hufton Aeronautical Department Royal Aircraft Establishment Farnborough, England
1	Paul F. Brinich NACA, Lewis Flight Propulsion Lab Cleveland 11, Ohio
1	Dr. I. I. Glass Institute of Aerophysics University of Toronto Toronto 5, Ontario, Canada
1	Prof. H. F. Ludloff Daniel Guggenheim School of Aeronautics New York University New York 3, New York
1	John Laufer Jet Propulsion Laboratory California Institute of Technology 4800 Oak Grove Drive Pasadena 2, California
1	William H. Dorrance Consolidated Vultee Aircraft Corporation San Diego, California
1	Professor Dean MIT, Gas Turbine Laboratory Engineering Department Cambridge, Massachusetts

No. of Copies	
1	Major J. B. Robinson U. S. Air Force Main Navy Building, Rm. 3816 Washington 25, D. C.
1	D. R. Bartz Jet Propulsion Laboratory California Institute of Technology 4800 Oak Grove Drive Pasadena 3, California
1	William F. Brown Los Alamos Scientific Laboratory University of California P. O. Box 1663 Los Alamos, New Mexico
1	P. S. Klebanoff Aerodynamic Section National Bureau of Standards Washington 25, D. C.
1	Judson Baron Naval Supersonic Laboratory Massachusetts Institute of Technology Cambridge, Massachusetts
1	Marvin Sweeney, Jr. Naval Supersonic Laboratory Massachusetts Institute of Technology Cambridge, Massachusetts
1	Dr. F. Frenkiel Applied Physics Laboratory The Johns Hopkins University 8621 Georgia Avenue Silver Spring, Maryland
1	Dr. F. K. Hill Applied Physics Laboratory The Johns Hopkins University 8621 Georgia Avenue Silver Spring, Maryland
1	Mr. E. A. Bonney Applied Physics Laboratory The Johns Hopkins University 8621 Georgia Avenue Silver Spring, Maryland

No. of Copies	
1	Dr. Francis R. Hama Institute of Fluid Dynam University of Maryland College Park, Maryland
1	Prof. S. F. Shen Aeronautical Engr. Dept University of Maryland College Park, Maryland
1	Prof. S. I. Pai Institute of Fluid Dynam University of Maryland College Park, Maryland
1	Dr. William Bollay Aerophysics Development C 15304 Sunset Blvd. Pacific Palisades, Califor
1	Dr. D. R. Chapman NACA, Ames Aeronautical L Moffett Field, California
1	Alvin Seiff NACA, Ames Aeronautical L Moffett Field, California
1	Morris W. Rubesin NACA, Ames Aeronautical L Moffett Field, California
1	R. G. Deissler NACA, Lewis Flight Propul Cleveland 11, Ohio
1	Coleman Du P. Donaldson 247 Nassau Street Princeton, New Jersey
1	R. J. Monaghan Aeronautical Department Royal Aircraft Establishm Farnborough, England
1	Satish Dhawan California Institute o Pasadena 4, Californ